



A Journal of



Accepted Article

Title: Palladium-based Catalysts Supported by Unsymmetrical XYC-1 Type Pincer Ligands: C5 Arylation of Imidazoles and Synthesis of Octinoxate Utilizing Mizoroki-Heck Reaction

Authors: Ankur Maji, Ovender Singh, Sain Singh, Aurobinda Mohanty, Pradip K Maji, and Kaushik Ghosh

This manuscript has been accepted after peer review and appears as an Accepted Article online prior to editing, proofing, and formal publication of the final Version of Record (VoR). This work is currently citable by using the Digital Object Identifier (DOI) given below. The VoR will be published online in Early View as soon as possible and may be different to this Accepted Article as a result of editing. Readers should obtain the VoR from the journal website shown below when it is published to ensure accuracy of information. The authors are responsible for the content of this Accepted Article.

To be cited as: *Eur. J. Inorg. Chem.* 10.1002/ejic.202000211

Link to VoR: <http://dx.doi.org/10.1002/ejic.202000211>

WILEY-VCH

FULL PAPER

Palladium-based Catalysts Supported by Unsymmetrical XYC^{-1} Type Pincer Ligands: C5 Arylation of Imidazoles and Synthesis of Octinoxate Utilizing Mizoroki-Heck Reaction

Ankur Maji, Ovender Singh, Sain Singh, Aurobinda Mohanty, Pradip K Maji*^[b] Kaushik Ghosh*^[a]

Dedication ((optional))

Abstract: A series of new unsymmetrical (XYC^{-1} type) palladacycles (**C1-C4**) were designed and synthesized with simple anchoring ligands L^1-H ($L^1H= 2-((2-(4-methoxybenzylidene)-1-phenylhydrazinyl)methyl)pyridine$, $L^2H= N,N$ -dimethyl-4-((2-phenyl-2-(pyridin-2-ylmethyl)hydrazono)methyl)aniline, $L^3H= N,N$ -diethyl-4-((2-phenyl-2-(pyridin-2-ylmethyl)hydrazono)methyl)aniline and $L^4H= 4-(4-((2-phenyl-2-(pyridin-2-ylmethyl)hydrazono)methyl)phenyl)morpholine$ $H=$ dissociable proton). Molecular structure of catalysts (**C1-C4**) were further established by single X-ray crystallographic studies. The catalytic performance of palladacycles (**C1-C4**) was explored with the direct Csp^2-H arylation of imidazoles with aryl halides derivatives. These palladacycles were also applied for investigating of Mizoroki-Heck reactions with aryl halides and acrylate derivatives. During catalytic cycle in situ generated Pd(0) nanoparticles were characterized by XPS, SEM and TEM analysis and possible reaction pathways were proposed. The catalyst was employed as a pre-catalyst for the gram-scale synthesis of octinoxate which is utilized as a UV-B sunscreen agent.

Introduction

Organic syntheses and chemical processing require highly effective (high turnover number i.e. TON) transition-metal based catalysts because it allows the use of minimum amounts of toxic or might be precious transition metals.^[1] Organometallic palladium complex catalyzed C-C bond-

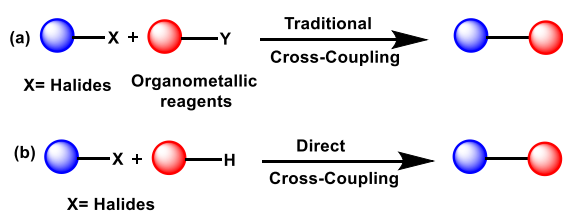
forming reactions are essential and frequently exploited in syntheses of pharmaceuticals and organic materials on both in laboratories as well as in industry.^[2] Several functionalized organometallic palladium complexes have been reported for various reactions namely hydrogenations,^[3] hydrophosphinations,^[4] C-H functionalization,^[5] Hiyama reaction,^[6] Suzuki-Miyaura reactions,^[7] Sonogashira coupling reactions^[8] Mizoroki-Heck reactions^[9] and Buchwald-Hartwig reactions^[10] etc.

The arylation of C-H bond of heterocycles, such as imidazole derivatives are imperative as they construct the building blocks of various biological and pharmaceutical compounds.^[11] The selective C-5 arylation of 1-methyl-1H-imidazole or 1,2-dimethyl-1H-imidazole with aryl halides to obtain 5-arylated 1-methyl-1H-imidazole or 5-arylated 1,2-dimethyl-1H-imidazole derivatives respectively have been established by using palladium-based catalysts.^[12] Though these metal catalysts efficiently perform the arylation of imidazoles, very often harsh reaction conditions, strong bases and expensive phosphine-based ligands^[13] and NHC ligands^[14] were utilized for satisfactory conversion. Moreover, the stability of catalyst in the air as well as thermal stability, are significant concerns, which enforces the usage of high catalyst loading (more than 0.5 mol%) in many reactions. Recently Liu and co-workers reported bis(imino)acenaphthene (BIAN)-supported palladium complexes. Further, these complexes effectively catalyzed cross-coupling reaction of (hetero)aryl bromides with azoles at low palladium loading of 0.5 mol%.^[12b] Similar cross-coupling reaction was also reported by Lee and co-workers however they have utilized palladium carbene complexes featuring NHC/amidate/phenoxy donor atoms as catalyst (2 mol% of catalyst loading) in their reactions. Investigation of the literature indicated that palladium complexes derived from pincer-type ligands might be productive and robust catalysts for such direct cross-coupling reaction.^[15]

[a] A. Maji, O. Singh, S. Singh, A. Mohanty, Prof. K. Ghosh
Department of Chemistry, Indian Institute of Technology Roorkee
Roorkee 247667, Uttarakhand, India. E-mail: ghoshfcy@iitr.ernet.in,
kaushik.ghosh@cy.iitr.ac.in
Homepage: <https://www.iitr.ac.in/departments/CY/pages/People+Faculty+ghoshfcy.html>

[b] Dr. P. K. Maji
Department of Polymer and Process Engineering, Indian Institute of
Technology Roorkee Saharanpur Campus, Saharanpur UP 247001,
India, E-mail: pradip.fpt@iitr.ac.in
Homepage: https://www.iitr.ac.in/departments/PPE/pages/People+Pradip_K_Maji.html
Supporting information for this article is given via a link at the end of
the document. ((Please delete this text if not appropriate))

FULL PAPER



Scheme 1. Schematic representation of cross-coupling reaction.

On the other hand, palladium-catalyzed Mizoroki-Heck reaction of aryl halides with alkenes is another pathway for C–C bond-forming processes in synthetic and medicinal chemistry.^[9] Palladacycles are effectively used in the Mizoroki-Heck reaction.^[9a,16] The performance of these metal catalysts are useful in reaction, but sometimes punitive reaction conditions and costly phosphine-based ligands^[17] are essential for satisfactory conversion. Uozumi and co-workers reported NNC-pincer based palladium complex as catalyst for Mizoroki-Heck reaction of aryl halides (iodides, bromides, or chlorides).^[9a] The present challenge for palladium-catalyzed coupling reactions demands novel catalysts with high-performance utilizing environmentally benign and sustainable reaction conditions. These reports prompted us to study Mizoroki-Heck reaction exploring newly synthesized palladacycles with a catalyst loading of as low as 0.001 mol%.

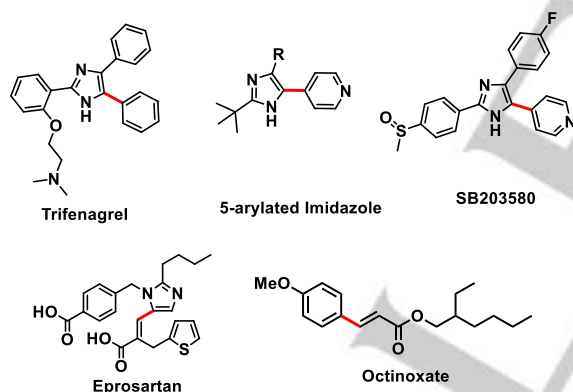


Figure 1. Some of biological active scaffolds.

Screening of literature, only a single report where palladium-based catalyst efficiently catalyzed C-5 arylation of imidazole (catalyst loading 2.5 mol%) derivatives as well as Mizoroki-Heck (catalyst loading 0.5 mol%) reaction.^[18] However, pincer based comparatively less explored for such C-5 arylation of imidazole derivatives as well as Mizoroki-Heck reaction (Scheme 1). Pincer ligands are in general symmetrical XC^{-1}X type (X = neutral donor) however, unsymmetrical ligand frames such as XC^{-1}Y and XYC^{-1} (X, Y = neutral donor) are also known in the literature.^[19] Pd–C σ -bond plays a crucial role in terms of

potential hemilability and thermal stability of the catalyst and exhibits better catalytic activity.^[20] Unsymmetrical pincer palladacycles are comparatively novel, however, the synthesis of their respective ligands often possess difficulty than their symmetrical ligands.^[9d]

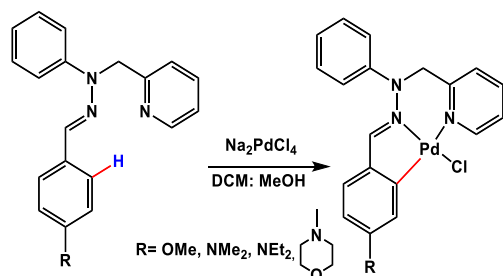
Imidazole derivatives exhibit a broad spectrum of biological and pharmacological activities.^[21] Trifenagrel having 5-arylated imidazole moiety is a potent arachidonate cyclooxygenase (COX) inhibitor. 5-arylated imidazole derivatives is an important scaffold present several biologically active molecules. For example, SB203580 is a potent anti-cancer agent. Eprosartan, which also contain 5-arylated imidazole ring is utilised as an angiotensin II receptor antagonist.^[22] Octinoxate (2-ethylhexyl-4-methoxycinnamate), which is an essential organic molecule utilized for UV-B sunscreen agent (shown in Figure 1).^[9a]

In recent years organometallic palladium-based catalysts were explored as a pre-catalyst for several C-H bonds activating reactions.^[9a,23] In most of these cases, Pd(0) nanoparticles were active species for such organic conversion. The anchoring ligands to palladium play important role in the stabilization of Pd(0) nanoparticles.^[7d,9a,24] Most of the ligands in this regard are combination of phosphorous, sulphur and selenium based organometallic complexes, however, NNC based pincer-type ligands were less explored for such Pd(0) nanoparticles based organic transformation.^[7d,24] These types of in-situ generated Pd(0) nanoparticles familiarized a new era of C5 arylation of imidazole derivatives.

Hence investigation of literature reports clearly expresses that palladacycles supported by pincer-type ligand would be interesting to explore novel reactivity studies. Herein we report the synthesis of palladacycles (**C1–C4**) and their characterization by IR, NMR, ESI-MS and single-crystal X-ray diffraction. These complexes were utilized for C5 arylation of imidazole derivatives as well as Mizoroki-Heck reactions with aryl halide (bromides, or chlorides). A total of 24 and 36 substrates were tested for C5 arylation of imidazole derivatives and Mizoroki-Heck reactions respectively. With the knowledge and lessons gained in the present study, we tried to synthesize octinoxate (2-ethylhexyl-4-methoxycinnamate), which is an essential organic molecule utilized for UV-B sunscreen agent. They are useful as homogeneous catalysts towards C5 arylation of imidazole derivatives and Mizoroki-Heck reactions. In the present study, we have also tried to propose a possible

FULL PAPER

reaction mechanism. Generation of Pd(0) nanoparticles during the catalytic reaction was authenticated by XPS analysis, TEM analysis, SEM analysis, hot filtration test and Hg, PPh₃ poisoning test.



Scheme 2. Schematic representation of synthesized palladacycles (**C1–C4**)

Results and discussion

Synthesis of ligands

Ligands L¹H–L⁴H were synthesized by condensation of corresponding benzaldehyde derivatives and 2-(1-(2-((1-phenylhydrazinyl)methyl)pyridine) in equimolar ratio respectively in methanol.^[25] After 8 hours, white-colored precipitate of ligands L¹H–L⁴H was obtained and characterized by several spectroscopic techniques. The IR spectra of the ligands show strong vibration observed at 1590–1596 cm⁻¹ in the ligands corresponding to $\nu_{C=N}$ of Schiff bases (shown in supporting information Figure S3–S6).^[25b] The ¹H-NMR spectra of the ligands show the signals in the expected regions.^[25b] The ¹H-NMR signal of –CH₂– group for all the ligand (L¹H–L⁴H) shows one singlet around 5.24 ppm (shown in supporting information Figure S11–S17). Positive mode ESI-MS spectra in acetonitrile exhibited m/z peaks 318.1998 (L¹H+H)⁺ ion for L¹H, 330.2189 (L²H)⁺ for L²H, 359.2348 (L³H+H)⁺ ion for L³H

and 371.2356 (L⁴H–H)⁺ ion for L⁴H respectively (shown in supporting information Figure S24–S27).

Catalysts design

Palladacycles (**C1–C4**) were synthesized using Na₂[PdCl₄] and neutral ligand L¹H, L²H, L³H and L⁴H in the equimolar ratio in dichloromethane and methanol solvent at room temperature (Scheme 2). Coordination of ligands with the metals was analyzed based on IR, NMR and ESI spectral studies. During IR spectral studies coordination of the nitrogen to the metal center resulted in a shift in the stretching frequency of $\nu_{(-HC=N)}$ in the range of 1576–1588 cm⁻¹. (shown in supporting information Figure S7–S10). It indicates the possible ligation to metal centers in all the palladium complexes. The ¹H-NMR signal of –CH₂– group for all the catalysts (**C1–C4**) was shifted from ~5.24 ppm to ~4.81 ppm due to the metal-ligand incorporation. Also, the doublet peak of pyridine center shifted from ~8.63 ppm to 9.37 ppm.^[25c] (depicted in supporting information Figure S18–S23). ESI-MS analysis of all the catalysts was recorded in acetonitrile shows molecular ion peak with the loss of a chloride ion. Positive mode ESI-MS spectra in acetonitrile exhibited m/z peaks 422.0542 [Pd(L¹–Cl)]⁺ for **C1**, 435.0786 [Pd(L²–Cl)]⁺ for **C2**, 463.1169 [Pd(L³–Cl)]⁺ for **C3** and 477.1173 [Pd(L⁴–Cl)]⁺ for **C4** respectively. (depicted in supporting information Figure S28–S31).

Structural studies

Even though the analytical and spectral data gave some ideas about the molecular formulae of the complexes, they do not provide precise coordination. Yellow-colored crystals of complexes **C1–C4** were obtained by slow evaporation of

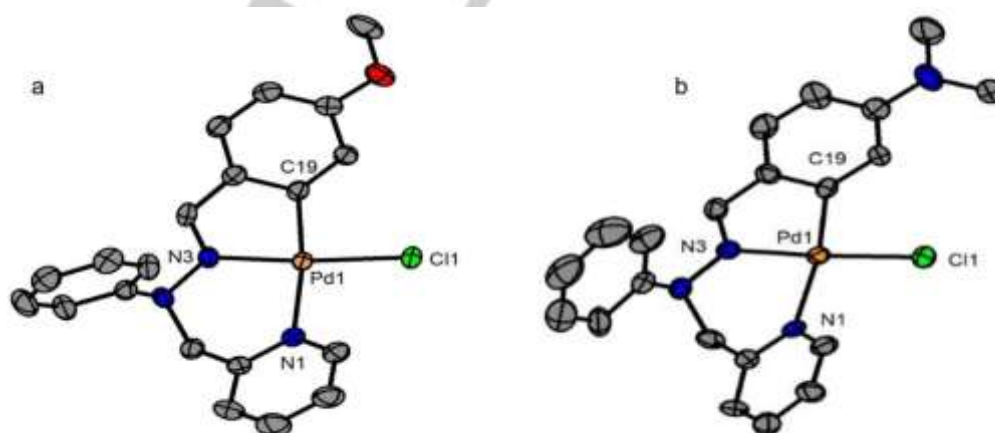


Figure 2. ORTEP plot (30% probability level) of (a) palladacycles **C1** and (b) palladacycles **C2**. Hydrogen atoms are not shown for clarity.

FULL PAPER

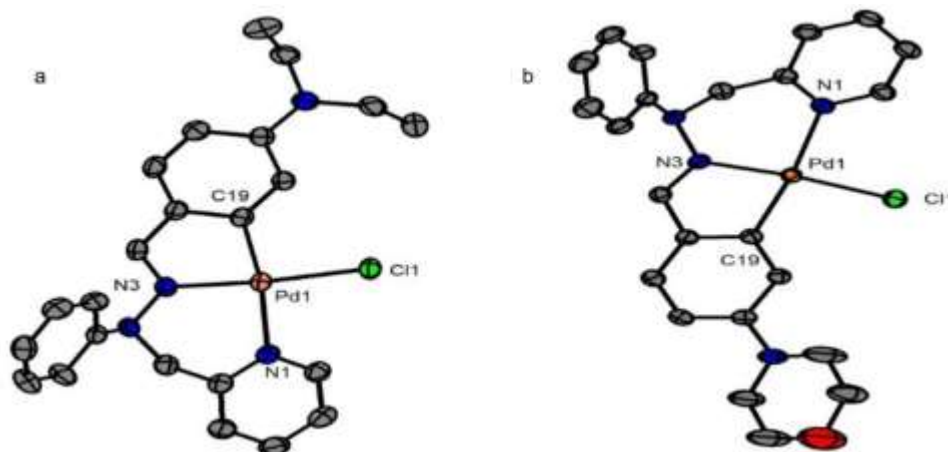


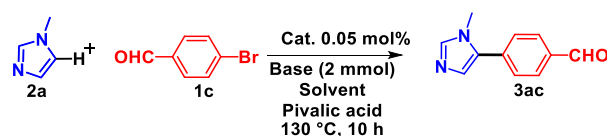
Figure 3. ORTEP plot (30% probability level) of (a) palladacycles **C3** and (b) palladacycles **C4**. Hydrogen atoms are not shown for clarity.

complexes in dichloromethane and hexane mixture (1:4) at room temperature within a week. The solid-state structure of complexes **C1-C4** was determined by single X-ray crystallography. The crystal data and structure refinement parameters for complexes **C1-C4** are summarized in Tables S2-S3 and selected bond lengths and bond angles are depicted in Tables S4-S7. The ORTEP view of complexes **C1-C4** given in Figures 2–3. The structures confirm that the ligands L¹H-L⁴H are coordinated to the palladium center in the targeted NNC fashion and another site co-ordinates to chloride. A distortion from square planar geometry, probably due to the uncommon combination of 5- and 6-membered rings in the metal coordination sphere. Each structure consists of a palladium center surrounded by two nitrogens donor's atom one carbon belonging to tridentate ligands (L¹H-L⁴H) along with a monodentate chloride to complete a geometry best described as distorted square planar. The bond distances involving the donor atoms in L¹H-L⁴H with the Pd(1)–N3 2.007(10) (Å), 2.006(10) (Å), 2.004(4) (Å) and 1.993(6) (Å) which is lower compared to the reported by Sun and coworkers^[9d] but higher than Bhattacharya and co-workers.^[7c] The bond distances Pd(1)–N(1) 2.178(9) (Å) and 2.162(10) (Å), 2.165(11) (Å) and 2.180(6) (Å) respectively for complexes **C1-C4** is lower than the Dominguez and co-workers^[26] and higher than Sun and co-workers.^[9d] The bond distances Pd(1)–C(19) are 2.002(12) (Å), 2.001(11) (Å), 1.993(9) (Å), and 1.997(6) (Å) respectively for complex **C1-C4** which are higher than Solan and co-workers^[27] and comparable with Dominguez and co-workers^[26] This strong Pd–C bond would play a better anchoring role to palladium. The bond lengths of Pd1–Cl1

ranged between 2.307(4) (Å) for **C1**, 2.334(4) (Å) for **C2**, 2.320(6) (Å) for **C3** and 2.322(7) (Å) for **C4** in following the related CNN pincer palladacycles.^[9d,28] Complexes (**C2-C4**) display unusual short-range C–H/π, and halogen bonding interactions are observed for **C2**, **C3** and **C4** with distances of 2.713, 3.123 and 2.713 Å⁺ respectively, between adjacent molecules indicative of favorable Van der Waals interactions which give rise to a zigzag arrangement one-dimensional tape in the solid-state (Shown in supporting information Figure. S32-34).

C_{sp}²–H arylation of imidazoles derivatives

Initially, the reaction conditions for the arylation reaction of 4-bromobenzaldehyde (**1c**) with 1-methyl-1H-imidazole (**2a**) using the **C2** catalyst were optimized by varying the



Scheme 3. Optimization of direct C5 arylation of 1-methyl-1H-imidazole in the presence of palladacycles **C2**.

concentrations of the catalyst, base, and solvent (Scheme 3, shown in supporting information Figure S1). When a dimethylacetamide (DMA) solution containing 1 mmol of 4-bromobenzaldehyde, 1 mmol of 1-Methyl-1H-imidazole, 2 mmol of K₂CO₃, 0.03 mmol pivalic acid and 0.05 mol% of

Entry	Base	Solvent	% Yield
1	K ₂ CO ₃	Toluene	40

FULL PAPER

2	K ₂ CO ₃	NMP	45
3	K ₂ CO ₃	DMF	61
4	K ₂ CO ₃	DMSO	67
5	K₂CO₃	DMA	92
6	KOH	DMA	60
7	NaOH	DMA	67
8	Na ₂ CO ₃	DMA	85
9	NaOAc	DMA	69
10	KOAc	DMA	71
11	K ₃ PO ₄	DMA	49
12	NaHCO ₃	DMA	47
13	K ^t OBu	DMA	71
14	Et ₃ N	DMA	43
15	K ₂ CO ₃	DMA	0 ^a /0 ^b
16	K ₂ CO ₃	DMA	20 ^c

Reaction conditions: **C2** (0.05 mol%), 1a (1.0 mmol), 2a (1 mmol), base (2 mmol), Pivalic acid (0.03 mmol) solvent (2.0 mL), 130 °C, 10 h. ^aIn absent of catalyst **C2**. ^bIn presence of L²H. ^cIn present of Na₂PdCl₄ 0.05 mol%.

complex **C2** was heated at 130 °C in a sealed tube to give 4-(1-methyl-1H-imidazol-5-yl)benzaldehyde (**3ac**) in 92% isolated yield after column purification (Table 1, entry 5).

A control experiment performed for this reaction in the absence of catalyst **C2** showed no formation of 4-(1-methyl-1H-imidazol-5-yl)benzaldehyde (Table 1, entry 15). In the presence of only ligand, no formation **3ac** and only in the presence of Na₂PdCl₄ small conversion of **3ac**. (Table 1, entry 15, 16). This result shows that the ligand has a crucial role in the arylation reaction. Among the different bases, K₂CO₃ and Na₂CO₃ give rise promising results up to isolated yield 92% and 85%, respectively (Table 1, entry 5, 8). Remarkably, heating of the reaction mixture containing 0.05 mol% of catalyst **C2**, 1 mmol of 4-bromobenzaldehyde, 1 mmol of 1-methyl-1H-imidazole, 2 mmol of K₂CO₃ and 0.03 mmol pivalic acid at 130 °C for 10 h, provided 1a in 92% yield. We next performed different acid additive for arylation of imidazoles reaction.^[29] Among the different acid additives, pivalic acid found to be more promising results up to isolated yield 92%. (shown in supporting information Table S1) To explore the scope of the arylation reaction, several aromatic bromobenzenes were examined in the presence of catalysts **C1-C4** (Table 2). The reaction of simple bromobenzene and 1-methyl-1H-imidazole

occurred in the presence of 0.05 mol% of catalysts to give isolation of 1-methyl-5-phenyl-1H-imidazole (**3aa**) 81-90% yield (Table 2). The arylation of 1-methyl-1H-imidazole with 4-COCH₃, 4-CHO, 4-CN, 4-NO₂, 4-Cl, and 4-F bromobenzene afforded the corresponding arylated products good to excellent yield up to 80-96% (Table 2, **3ab-3ag**). Electron-rich bromobenzene derivatives 4-OMe, 4-Me and 3-OMe also reacted similarly with 1-methyl-1H-imidazole to obtain the corresponding products **3ah**, **3ai** and **3aj** in moderate yield 73% to 86% respectively. The possibilities of expanding this reaction for the synthesis of hetero and sterically hindered arylation were also explored by reacting 1-methyl-1H-imidazole with hetero and sterically hindered bromobenzene to the formation of 3-(1-methyl-1H-imidazol-5-yl)pyridine and 1-methyl-5-(naphthalen-1-yl)-1H-imidazole moderate yield in the presence of catalysts (**C1-C4**) up to 85% yield (Table 2, **3ak** and **3al**). The direct arylation substituted imidazole, 1,2-dimethyl-1H-imidazole with aryl and heteroaryl halides having various substituents (electron-rich, electron-deficient and sterically hindered). The C5-monoarylated imidazole was obtained as the predominant product (yield up to 96%) in the process catalyzed with **C1-C4**. (Table 2, **4aa-4al**). We also investigated the direct arylation substituted N-methyl imidazole and 1,2-dimethyl-1H-imidazole with aryl and heteroaryl chlorides having various substituents (electron-rich, electron-deficient and sterically hindered). The C5-monoarylated imidazole was obtained as the predominant product (yield up to 79%) in the process catalyzed with **C1**. A comparison of the catalytic properties of **C1-C4** reported in the recent past for direct arylation of aryl halides derivatives were investigated. Liu and co-workers^[30] reported Pd(II) complexes derived from bis(imino)acenaphthene-supported N-heterocyclic carbene (loading 0.5 mol%), which less effective compare to **C1-C4**. Lee and co-workers^[31] recently reported imidazopyridine-based abnormal carbene ligands based palladium catalyst (catalyst loading 0.5 mol%), which has less effect. Singh and co-workers^[32] synthesized N-Heterocyclic carbene amidates ligand-based palladium complexes, which also less effective. Mao *et al.*^[33] Pd/C as a the heterogeneous catalyst for direct arylation of imidazoles derivative catalyst loading 1 mol%. Among the reported catalysts, the reported catalysts by us are most active, additionally air-stable Schiff base as anchoring catalysts.

FULL PAPER

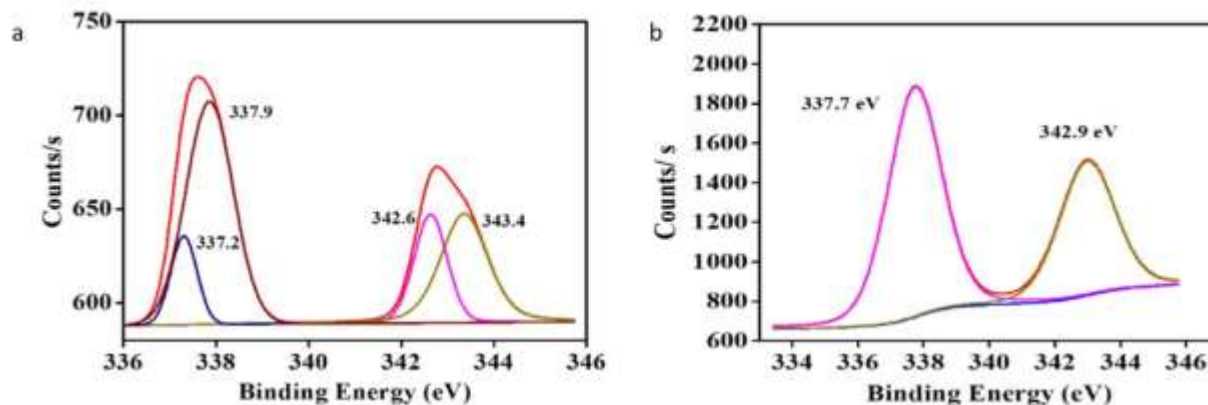


Figure 4. XPS spectra of the 3d level of palladium and deconvolution peaks of the Pd species: experimental (light grey), deconvoluted (red), Pd(II) (wine and dark yellow), Pd(0) (navy, magenta), (a) precatalyst **C2** (b) Precatalyst **C2** after treatment with K_2CO_3 , 4-bromobenzaldehyde with 1-methyl-1H-imidazole in DMA at 140 °C after 4h.

Probable mechanism

During the progress of direct arylation reactions, black particles develop into the surface of the reaction vials. It might be existing palladacycles (**C1-C4**) are not real catalysts. In situ formation of palladium nanoparticles (Pd NPs) has also been recognized in many cases during the catalytic process.^[34] Thus reactions of 4-bromobenzaldehyde with 1-methyl-1H-imidazole in DMA catalyzed with **C2** under optimum conditions have been examined in detail to explain the nature of black particles produced in situ during the catalytic pathway. To confirm the same, X-ray photoelectron spectroscopy (XPS) study has been performed of the catalyst as well as the reaction mixture of the direct arylation reaction. The surface compositions of palladium species (shown in Figure 4). 3d core-level palladium of complex **C2** fitted with two main peaks, where the Pd 3d_{5/2} and 3d_{3/2} peak at 342.9 eV and 337.7 eV was assignable to the Pd(II) species.^[35] To characterize the intermediate species generated during direct arylation reaction XPS analysis was inspected in the presence of catalyst **C2**. The dominant Pd 3d_{5/2} peak shifted to the binding energy at 343.4 eV from 342.9 eV and 3d_{3/2} peak shifted at 337.9 eV from and 337.7 eV which could be assigned to new Pd(II) species. Two different new peaks at 342.6 eV and 337.2 eV which consigned Pd 3d_{5/2} and Pd 3d_{3/2} of Pd(0) species.^[35,36] This peak confirms that both Pd(II) and Pd(0) species were involved during the catalytic cycle. TEM analysis of the reaction mixture after the reaction in the presence of catalyst **C2**. Palladium nanoparticles were observed in the reaction mixture (Figure 5). From the size distribution curve, the average size of these nanoparticles was estimated to be 4-5 nm. SAED pattern

reveals the polycrystalline nature of palladium nanoparticles. Besides, Pd nanoparticles provide excellent surface-to-volume ratio, which significantly amplifies the proximity between reactants and catalyst. This experiment shows that the **C1-C4** is pre-catalyst of this catalytic cycle. To confirm the observations, Hg poisoning test was conducted. Under optimization reaction condition, in the presence of catalyst **C2**, 4-bromo benzaldehyde, 1-methyl-1H-imidazole, K_2CO_3 and pivalic acid in DMA solvent, we found [4-(1-methyl-1H-imidazol-5-yl)benzaldehyde a coupled product 33% after 10 h in the presence of 1 drop Hg. These results unambiguously proved a generation of ligandless palladium species which may be catalytically active species in this reaction. Assembling of observations from XPS, TEM, Hg poisoning test and literature, a probable mechanistic pathway can be sketched out (shown in Scheme 4). Palladium complexes (**C1-C4**) were the pre-catalysts which form the palladium(0) species or palladium(0) clusters in the equilibrium under the reaction conditions ($A' \rightleftharpoons A''$).^[16a,34] Due to the in-situ formation Pd nanoparticles during the arylation of imidazoles high surface area of Pd(0) or Pd(0) cluster shown excellent catalytic activity. Subsequently, oxidative addition of bromobenzene to give rise the intermediate B. The ligand exchange happens with potassium salts of pivalic acid provided intermediate C. The C-H bond (C5) cleavage step 1-methyl-1H-imidazole/1,2-dimethyl-1H-imidazole with the aid of pivalate generates intermediate C via CMD transition state^[34,37] which undergoes reductive elimination give rise to the arylated product and regenerates Pd(0) intermediate (A).

FULL PAPER

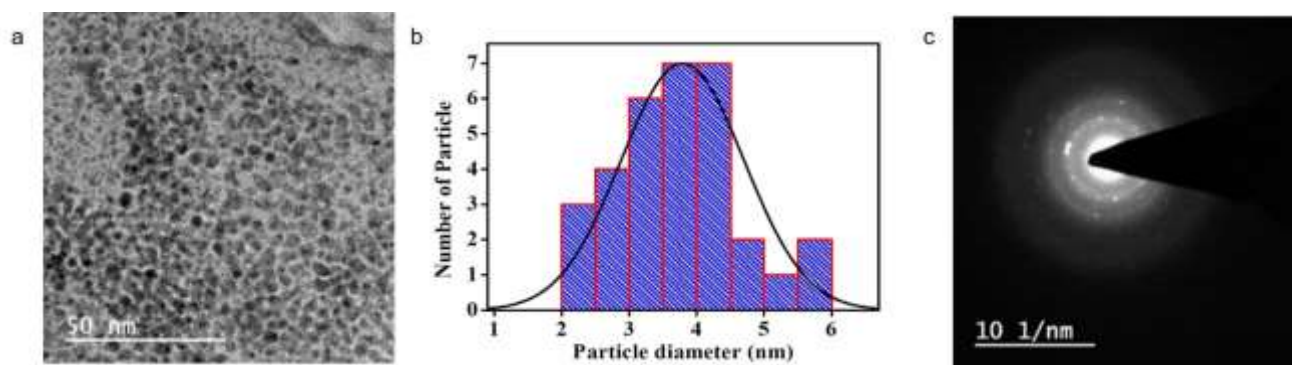
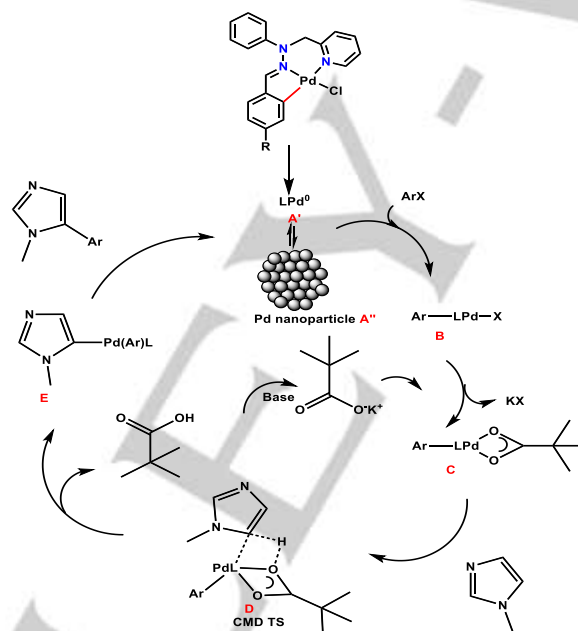


Figure 5. (a) TEM image of NPs obtained respectively during SMC (scale bar 50 and 20 nm). (b) The particle size distribution of spherical Pd nanoparticles obtained during C_{sp^2} -H arylation of imidazoles. (c) SAED pattern of NPs obtained during the catalysis



Scheme 4. Probable reaction pathway of C-H activation of imidazole derivatives.

Mizoroki-Heck reactions



Scheme 5. Optimization of Mizoroki-Heck coupling in the presence of palladacycles **C2**.

Nitrogen-based ligands are economical and air-stable, unlike phosphine-based ligands.^[1b] Simple synthesis, stability and smooth

handling of non-phosphine cyclometalated palladium complexes are accountable for their universality and rising importance in catalysis.

We explored the synthesized palladacycles (**C1**- **C2**) for Mizoroki-Heck coupling reactions (Scheme 5). For the optimization of catalyst, **C2** as a model catalyst has been chosen.

Entry	Base	Solvent	% Yield
1	K_2CO_3	NMP	21
2	NaOAc	NMP	37

FULL PAPER

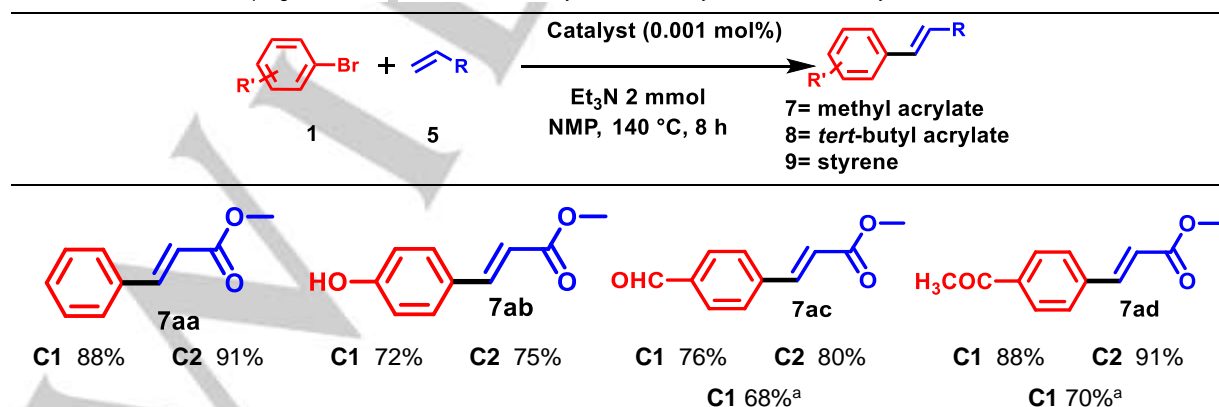
3	Na ₂ CO ₃	NMP	53
4	Et ₃ N	NMP	92
5	NaOH	NMP	49
6	KOH	NMP	43
7	KOAc	NMP	33
8	Et ₃ N	DMF	77
9	Et ₃ N	Toluene	71
10	Et ₃ N	DMSO	75
11	Et ₃ N	NMP	0 ^a /0 ^b
12	Et ₃ N	NMP	31 ^c

Reaction conditions: 1.0 mmol aryl halides, 1.2 mmol arene, 2 mmol Base, 0.001 mol% Pd(II) **C2**, 140 °C, 8 h. solvent: 2 mL, ^aIn absent of catalyst **C2**. ^bIn presence of L²H. ^cIn present of Na₂PdCl₄ 0.05 mol%.

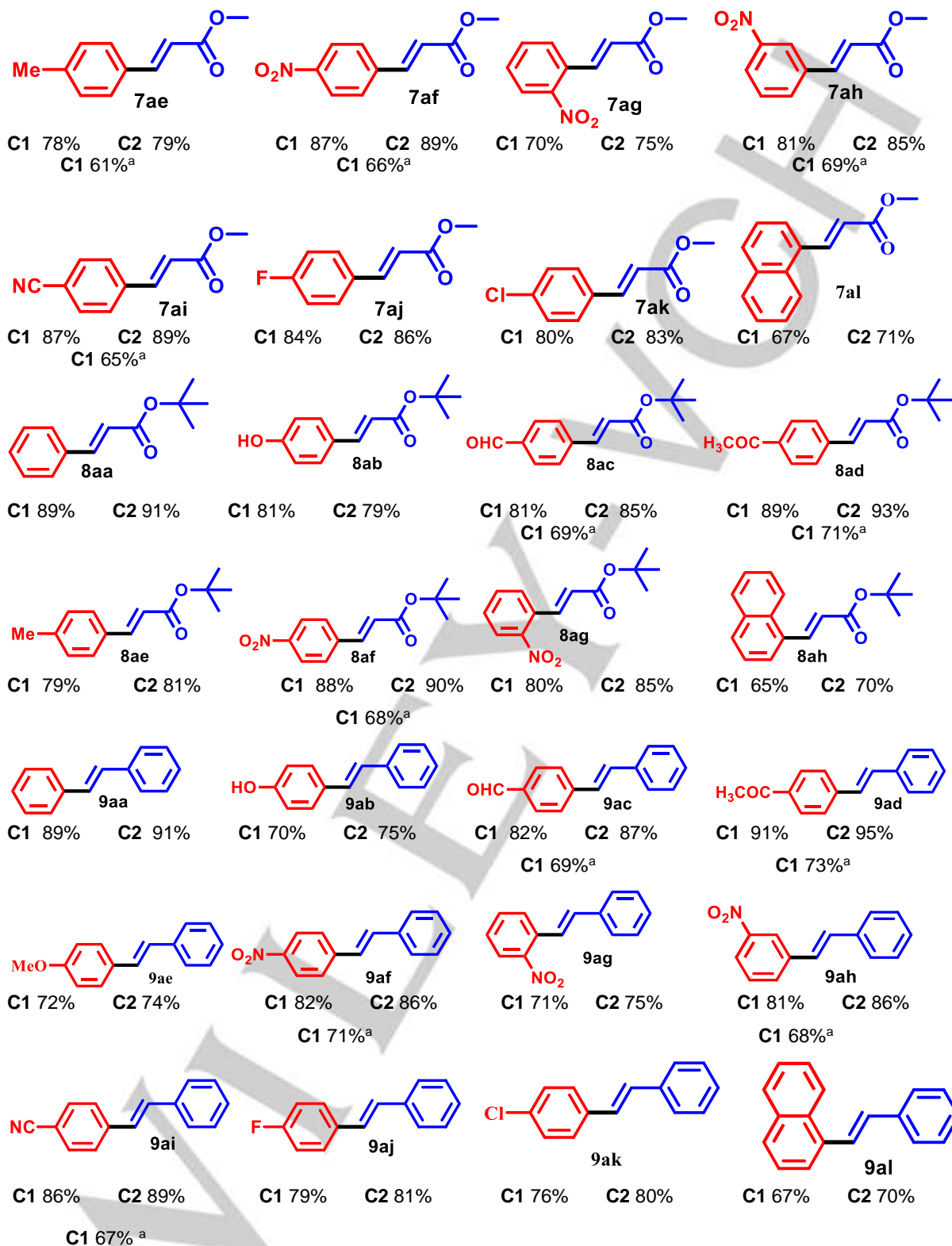
The most appropriate reaction parameters have been found when the coupling was performed in N-methyl-2-pyrrolidone (NMP) at 140 °C in the presence of triethylamine (Et₃N) for 8 h resulting in a 92% conversion of methyl acrylate (Table 3, entry 4). Some other solvent like dimethylformamide (DMF), toluene and dimethyl sulfoxide (DMSO) also examined similar conditions, but these all proved less effective (Table 3, entry 8-10). Control experiments revealed that the Mizoroki-Heck coupling reaction does not proceed in the presence of only ligand (L²H) and absent of **C2** (Table 4, entry 11). Commonly available palladium(II)-salt Na₂PdCl₄ were also found to be ineffective (Table 4, entries 12). These control experiments suggest that the catalyst has an essential role in such coupling reaction. As expected, using more activated arenes led to higher conversions. Based on the promising results obtained for the Mizoroki-Heck coupling of bromobenzene with methyl acrylate, it has been decided to explore the potential of **C1** and **C2** for the coupling reaction of other haloarenes with methyl acrylate, tert-butyl acrylate and styrene, the results are summarized in Table 4. Under the

optimization condition, it has been found that electron-deficient arenes such as 4-COCH₃, 4-CHO, 4-NO₂, 4 -CN, 4-F, 4-Cl) bromobenzene (Table 4, **7ac**, **7ad**, **7af**, **7ai-7ak**) effectively converted corresponding cross-coupled product in a higher yield as well as higher turnover number (TONs) yield up to 91%. However, when electron-rich halo arene 4-OH and 4-CH₃ (Table 4, **7ab**, **7ae**) introduced, the effectively converted corresponding cross-coupled product with moderate yield upto 79%. This catalyst also effectively converted 3-NO₂ and 2-NO₂ bromobenzene corresponding coupled product good to moderate yield 70% to 85% (Table 4, **7ag**, **7ah**). Sterically hindered 2-naphthylbromobenzene gives rise to moderate yield 61% to 69%. Heteroarene, like 3-bromopyridine, also afforded good to moderate yield 75%-83% (Table 4, **7al**). The coupling reaction of other haloarenes with tert-butyl acrylate give rise to good to excellent result (Table 4, **8aa-8ah**). When styrene used reaction with bromobenzenes proceeded smoothly to give the corresponding stilbenes derivative in good yields. On the other hand, bromobenzenes containing electron-rich and electron-poor offer the corresponding stilbene derivatives in moderated yields. (Table 4, **9aa-9al**). The coupling reaction of other hetero-haloarenes with tert-butyl acrylate give rise to good to excellent result (Table 4, **10aa-10ac**). Mizoroki-Heck reactions of arenes with aryl chloride derivatives also effective give rise to good to moderate yield up to yield 73% in the presence of **C1**. The catalytic properties of **C1-C2** with catalysts reported in the recent past for the Mizoroki-Heck reactions with aryl halides derivatives were investigated. Uozumi and co-workers reported^[38] Pd(II) complexes derived from

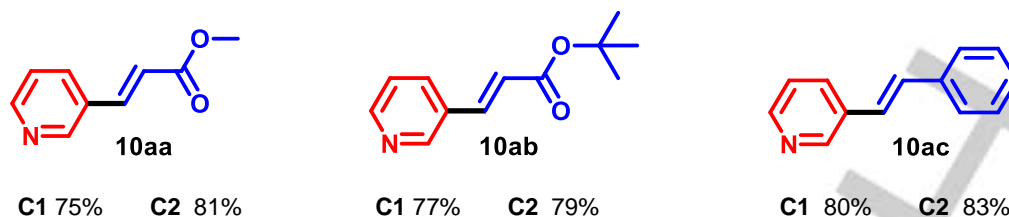
Table 4. Mizoroki-Heck coupling of **C1** and **C2** with functionalized aryl halides and acrylate derivatives and styrene.



FULL PAPER



FULL PAPER



Reaction conditions: 1.0 mmol aryl halides, 1.2 mmol arene, 2 mmol Et₃N, 0.001 mol% Pd(II) cat., 140 °C, 8 h. ^aaryl chloride derivatives.

NCN (0.0001 mol% catalyst loading) in the reaction mixture; however, in this report, only iodoarene derivatives were utilized. Sun and co-workers recently reported unsymmetrical CNN-palladacycles ligands^[9d] (catalyst loading 0.002 mol%) though in this report, bromoarene and iodoarene derivatives were exploited, less effective compare to **C1-C2**.

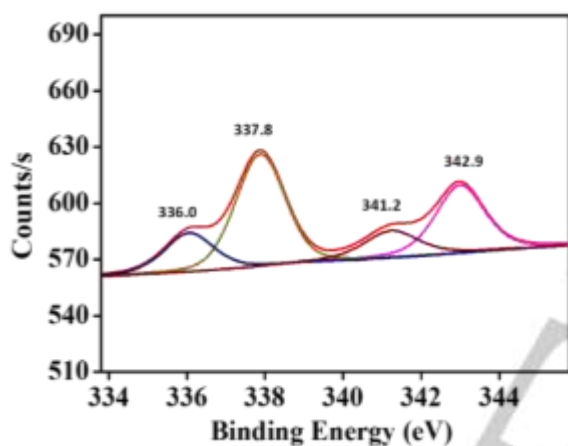


Figure 6. XPS spectra of the Pd 3d level and deconvolution peaks of the Pd species: deconvoluted (red), Pd(II) (magenta and navy), Pd(0) (dark yellow and wine) precatalyst **C2** after treatment with Et₃N, arene and bromobenzene in NMP at 140 °C after 8h

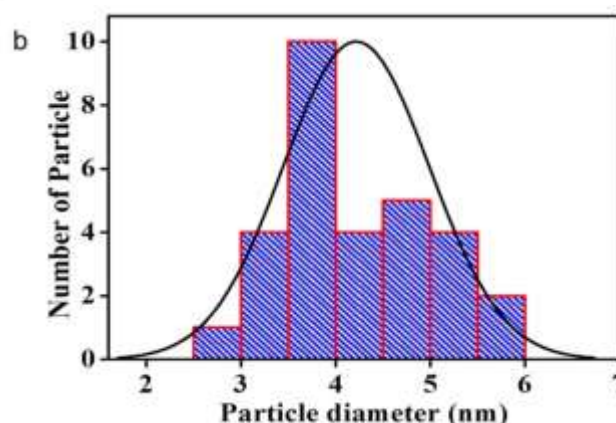
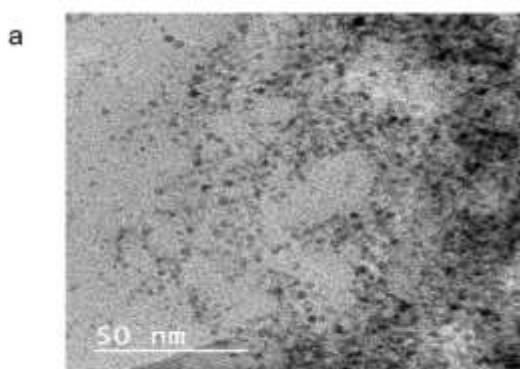


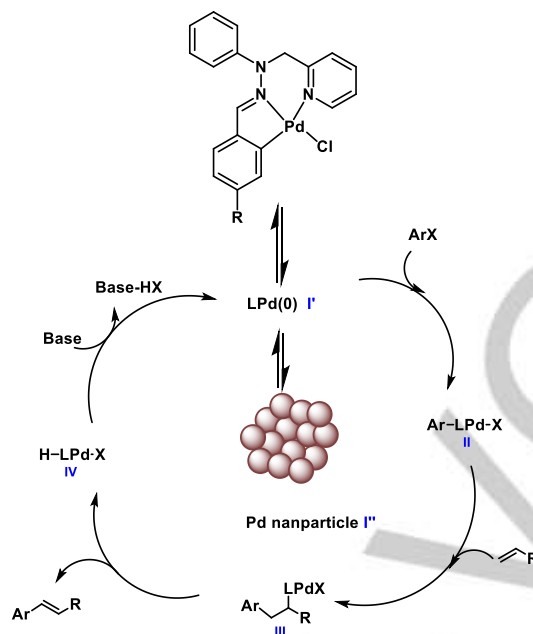
Figure 7. (a) TEM image of NPs obtained respectively during SMC (scale bar 50). (b) The particle size distribution of spherical Pd nanoparticles obtained during precatalyst **C2** after treatment with Et₃N, methyl acrylate and bromobenzene in NMP at 140 °C after 8h.

Uozumi and co-workers synthesized NNC-Pincer ligand-based palladium^[9a] complexes (catalyst loading 10 mol ppm), which comparatively effective than **C1-C2**. However, they utilized bromoarene, iodoarene chloroarene derivatives. Xiao and co-workers (N,C,N)^[9c] pincers having a bis(azole) ligand-based palladium complexes (catalyst loading 0.1 mol%) for coupling reaction utilized bromoarene, iodoarene derivatives. However, with **C1** and **C2**, Mizoroki-Heck reactions in good yield are achieved with 0.001 mol% loading of catalyst at 140 °C in 8 h. Additionally, chlorobenzene derivatives also effectively coupled with different acrylate derivatives in the presence of catalyst **C2** (catalyst loading 0.001 mol%).

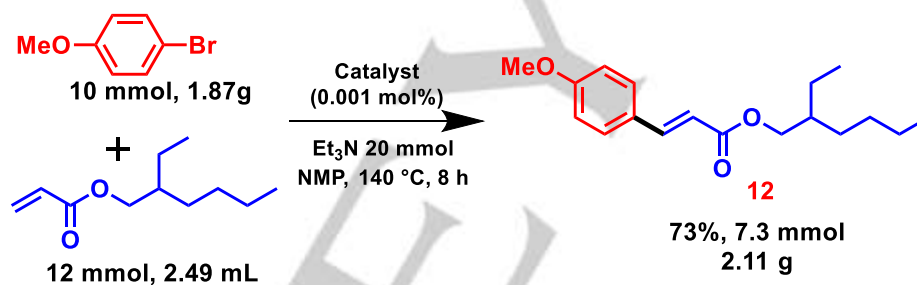
Probable reaction pathway

The catalytic pathway of the Mizoroki-Heck reactions. For the establishment of the reaction cycle, we did Hg poisoning test, under the standard reaction condition, the addition of mercury (1 drop) to the reaction mixture, after 8 hours, when the yield of **4aa** was 15%, significantly impeded the reaction. This reaction exposes that the ligandless monomeric palladium species and or palladium cluster may be palladium nanoparticles involves in the reaction mixture. Next, we

FULL PAPER



Scheme 6. Probable mechanism of Mizoroki-Heck reactions



Scheme 7. Gram-scale synthesis of octinoxate.

performed XPS analysis of the reaction mixture under the standard condition in the presence of catalyst **C2** (shown in Figure 6). We found four peaks at 336.0 eV and 337.8 eV, 341.2 and 342.9 eV, which assigned of Pd(0) and Pd(II) are present in the reaction mixture.^[36,37] Further, TEM analysis of the reaction mixture in the presence of palladium complexes **C2** we observed palladium nanoparticle. (shown in Figure 7). From the size distribution curve, the average size of these nanoparticles was estimated to be 3.5 nm to 4.5 nm.^[9a] This data indicates that the active surface area of the reaction mixture is very high and showed excellent catalytic activity. On the above experimental finding and literature under the elevated temperature and basic reaction conditions, palladacycle (**C2**) undergoes reduction. It provides a catalytically active Pd(0) complex with the cleavage of the Pd–C bond.^[39] The catalytic efficiencies of these release

nanoparticles Pd(0) species are finely tuned of the reactivity/selectivity of the catalytic reaction by ligands (here L¹H–L⁴H).^[16,40]

Therefore catalysts **C1–C4** are a precursor of the actual catalytically active species in this reaction. Based on literature reports and experimental findings at first, the palladium(II) precatalyst has to be reduced to palladium(0) nanoparticles or palladium(0) cluster in the equilibrium under the reaction conditions ($I' \rightleftharpoons I''$) to enter the catalytic cycle. After that, the oxidative addition of bromobenzene occurred and the formation of intermediate **II**. Followed by migratory insertion happens formed intermediate **III**. Then β -elimination happens and formed the coupled products and intermediate **IV**. In the presence of base regenerate the catalyst Pd(0) or palladium(0) clusters and continue the reaction cycle. (shown in Scheme 6).

FULL PAPER

Gram-scale synthesis of the UV-B sunscreen agent octinoxate

Importantly, the current methodology could be utilized to directly prepare a gram-scale synthesis of the UV-B sunscreen agent octinoxate (2-ethylhexyl(E)-3-(4-methoxyphenyl) acrylate) (Scheme 7). The reaction of 1-bromo-4-methoxybenzene (10 mmol) and 2-ethylhexyl acrylate (12 mmol) give rise to (2-ethylhexyl(E)-3-(4-methoxyphenyl) acrylate) with 73% yield in the presence of catalyst **C2**.

Homogenous and heterogeneous test

To conclude whether the palladacycles is actually working in a heterogeneous manner, or whether it is merely a reservoir for more active soluble forms of Pd, various tests were performed. A hot filtration test confirmed the leaching of palladium species in both the catalytic reaction. In case of after 1 h, reaction was filtered and reaction further run additional conversion (from 37% (after 1h) to 88% (10 h) in case of arylation of imidazole and from 21% (after 1h) to 69% (8 h) in case of Mizoroki-Heck coupling in the presence of catalyst **C2**) was measured in the hot filtration test.^[41] This test suggested that the involvement of a homogeneous pathway. In the presence of 1 drop Hg, retardation of the catalytic process also indicated the palladacycles are a reservoir for more active soluble forms of Pd. PPh₃ poisoning test also conducted for the catalytic reaction gives rise to cross-coupled 31% and 41% yield of arylation reaction and Mizoroki-Heck coupling reaction, respectively. The results suggest that discrete Pd(0) nanoparticles generated in-situ in the reaction mixture it behaves like a homogenous catalysts.^[42]

Conclusion

A new family of palladacycles (**C1-C4**) derive from designed unsymmetrical XYC⁻¹ type pincer ligands were synthesized and characterized. These palladacycles were pre-catalysts for the Csp²-H arylation of imidazoles with aryl halides as well as Mizoroki-Heck reactions. The reactions offer advantages of operational simplicity, mild conditions, good to excellent yield, broad substrate scope low catalyst loading 0.05 mol% for arylation of imidazoles with aryl bromides (TON up to 1.9x10³) aryl chlorides bromides (TON up to 7.9x10²) and 0.001 mol% for Mizoroki-Heck reactions with aryl bromides (TON up to 9.5x10⁴) and with aryl chlorides (TON up to 7.3x10⁴). We tried to investigate the reaction pathway of the above reactions and found out the generation of Pd(0) nanoparticles in situ. Probable mechanisms established based on experimental as

well as reported literature. These palladacycles are potent catalysts for the gram-scale synthesis of UV-B sunscreen agent octinoxate. The successful synthesis of palladacycles could give inspiration in the development of efficient catalysts for direct transformation of C-H bond to C-C bond in organic transformation. Other catalytic studies of these palladacycles are under progress.

Experimental

The reported methods were used for the synthesis of 2-picolylphenylhydrazine.^[25] All aldehydes, Aryl bromides and chlorides, 1-methyl-1H-imidazole, 1,2-dimethyl-1H-imidazole, methyl acrylate, tert-butyl acrylate, styrene K₂CO₃ and were purchased from Avra, Himedia, TCI Chemicals (India) Pvt. Ltd. Solvents used for spectroscopic studies were HPLC grade and purified by standard procedures before use. Palladium chloride was obtained from Arora Matthey, Kolkata, India. Infrared spectra were recorded as KBr pellets on a Nicolet NEXUS Aligent 1100 FT-IR spectrometer, using 50 scans and are reported in cm⁻¹. Transmission electron microscopy (TEM, Tecnai G2 20SeTWIN, FEI Netherlands) was used for the morphological characterization of catalytically active species. ¹H-NMR and ¹³C-NMR spectra were measured with a Bruker AVANCE 500.13 MHz spectrometer and JEOL 400 MHz spectrometer, chemical shifts were reported in δ (ppm) units relative to tetramethylsilane (TMS) as an internal standard. Proton coupling patterns are described as singlet (s), doublet (d), triplet (t), quartet (q), multiplet (m), and broad (br). (ESI-MS) experiments were performed on a Bruker micrOTOFM-Q-II mass spectrometer.

X-ray crystallography

Yellow crystals of **C1-C4** were obtained by slow evaporation of solution from the complexes in dichloromethane and methanol. The X-ray data collection and processing for complexes were performed on a Bruker Kappa Apex-II CCD diffractometer by using graphite monochromated Mo-K α radiation ($\lambda = 0.71073$ Å) at 296 K for **C1**, 130 K for **C2**, 296 K for **C3** and 293 K for **C4**. Crystal structures were solved by direct methods. Structure solutions, refinement and data output were carried out with the SHELXTL program.^[43-45] All non-hydrogen atoms were refined anisotropically. Hydrogen atoms were placed in geometrically calculated positions and purified using a riding model. ORTEP diagrams were generated with the DIAMOND program.^[46]

FULL PAPER

Synthesis of L¹H

4-anisaldehyde (0.272 g, 2.00 mmol) and 2-((1-phenylhydrazinyl)methyl)pyridine (0.398 g, 2.00 mmol) were dissolved in 10 mL of methanol. The reaction mixture was stirred at room temperature. Within 1 h, a white solid began to separate and stirring was continued for another 3 h. The white precipitate was filtered, washed thoroughly with methanol, diethyl ether and then dried in vacuum and recrystallized in dichloromethane.

Selected IR data: (KBr, ν/cm^{-1}): 1590($\nu_{\text{C}=\text{N}}$). Anal. calcd for $\text{C}_{20}\text{H}_{19}\text{N}_3\text{O}$: C, 75.69; H, 6.03; N, 13.24 found C, 75.57; H, 6.12; N, 13.15. $^1\text{H-NMR}$ (500 MHz, CDCl_3) δ 8.63 (d, $J = 4.2$ Hz, 1H), 7.58 – 7.54 (m, 3H), 7.40 – 7.35 (m, 3H), 7.31 (t, $J = 8.0$ Hz, 2H), 7.20 – 7.16 (m, 1H), 7.08 (d, $J = 7.9$ Hz, 1H), 6.93 (t, $J = 7.2$ Hz, 1H), 6.86 (d, $J = 8.8$ Hz, 2H), 5.25 (s, 2H), 3.79 (s, 3H). $^{13}\text{C-NMR}$ (101 MHz, CDCl_3) δ 159.77, 150.03, 147.74, 137.31, 132.87, 129.31, 127.64, 122.52, 120.77, 120.66, 114.62, 114.10, 55.43, 52.27. ESI-MS: 318.1998 ($\text{L}^1\text{H}+\text{H}^+$)⁺ ion. Yield: 463.4, 73%.

Synthesis of L²H

L^2H was prepared by following the procedure described above for L^1H , instead of 4-anisaldehyde used 4-(dimethylamino)benzaldehyde (0.298 g, 2.00 mmol)

Selected IR data: (KBr, ν/cm^{-1}): 1596 ($\nu_{\text{C}=\text{N}}$). Anal. calcd for $\text{C}_{21}\text{H}_{22}\text{N}_4$: C, 76.33; H, 6.71; N, 16.96 found C, 76.25; H, 6.83; N, 16.84. $^1\text{H-NMR}$ (500 MHz, CDCl_3) δ 8.63 (d, $J = 4.2$ Hz, 1H), 7.54–7.50 (m, 3H), 7.40 – 7.36 (m, 3H), 7.30 (t, $J = 8.0$ Hz, 2H), 7.17 (dd, $J = 6.9, 5.2$ Hz, 1H), 7.08 (d, $J = 7.9$ Hz, 1H), 6.90 (t, $J = 7.2$ Hz, 1H), 6.68 (d, $J = 8.9$ Hz, 2H), 5.24 (s, 2H), 2.95 (s, 6H). $^{13}\text{C-NMR}$ (101 MHz, CDCl_3) δ 156.64, 150.59, 149.95, 147.90, 137.29, 133.97, 129.27, 127.52, 124.84, 122.44, 120.86, 120.19, 114.38, 112.35, 52.16, 40.59. ESI-MS: 330.2189 (L^2H^+)⁺ ion. Yield: 508.9 mg, 77%.

Synthesis of L³H

L^3H was prepared by following the procedure described above for L^1H , instead of 4-anisaldehyde used 4-(diethylamino)benzaldehyde (0.354 g, 2.00 mmol).

Selected IR data: (KBr, ν/cm^{-1}): 1595 ($\nu_{\text{C}=\text{N}}$). Anal. calcd for $\text{C}_{23}\text{H}_{26}\text{N}_4$: C, 77.06; H, 7.31; N, 15.63 found C, 77.15; H, 7.23; N, 15.51. $^1\text{H-NMR}$ (500 MHz, CDCl_3) δ 8.63 (d, $J = 4.5$ Hz, 1H), 7.54 (t, $J = 8.5$ Hz, 1H), 7.49 (d, $J = 8.8$ Hz, 2H), 7.40 – 7.35 (m, 3H), 7.30 (t, $J = 7.9$ Hz, 2H), 7.19 – 7.15 (m, 1H), 7.08 (d, $J = 7.9$ Hz, 1H), 6.90 (t, $J = 7.2$ Hz, 1H), 6.63 (d, $J = 8.8$ Hz, 2H), 5.24 (s, 2H), 3.35 (q, $J = 7.1$ Hz, 4H), 1.15 (t, $J = 7.1$ Hz,

6H). $^{13}\text{C-NMR}$ (101 MHz, CDCl_3) δ 156.73, 149.93, 147.96, 137.25, 134.19, 129.25, 127.79, 122.40, 120.88, 120.06, 114.33, 111.61, 52.12, 44.55, 12.68. ESI-MS: 359.2348 ($\text{L}^3\text{H}+\text{H}^+$)⁺ ion. Yield: 72% Yield: 544.9 mg, 76%.

Synthesis of L⁴H

L^4H was prepared by following the procedure described above for L^1H , instead of 4-anisaldehyde used 4-morpholinobenzaldehyde (0.382 g, 2.00 mmol).

Selected IR data: (KBr, ν/cm^{-1}): 1597 ($\nu_{\text{C}=\text{N}}$). Anal. calcd for $\text{C}_{23}\text{H}_{24}\text{N}_4\text{O}$: C, 74.17; H, 6.49; N, 15.04 found C, 74.09; H, 6.55; N, 14.78. $^1\text{H-NMR}$ (400 MHz, CDCl_3) δ 8.63 (d, $J = 5.6$ Hz, 1H), 7.56 (t, $J = 6.8$ Hz, 1H), 7.51 (d, $J = 8.8$ Hz, 2H), 7.40 – 7.34 (m, 3H), 7.33 – 7.27 (m, 2H), 7.21 – 7.15 (m, 1H), 7.08 (d, $J = 7.8$ Hz, 1H), 6.92 (d, $J = 7.2$ Hz, 1H), 6.88 (d, $J = 8.8$ Hz, 2H), 5.24 (s, 2H), 3.21 – 3.15 (m, 4H), 1.68 (m, 4H). ESI-MS: 371.2356 (L^4H^+)⁺ ion. Yield: 528.9 mg, 71%.

Syntheses of Complexes C1-C4

0.10 mmol of ligands ($\text{L}^1\text{H-L}^4\text{H}$) was stirred in 10 mL dichloromethane for 15 min. Methanolic solution of $\text{Na}_2[\text{PdCl}_4]$ (0.029 g, 0.10 mmol) [Na_2PdCl_4 was prepared in situ PdCl_2 (0.1 mmol and 6 equivalent NaCl stirred for 1 h)] were added to it. The mixture was stirred further for 6 h at room temperature. The yellow color solid formed was collected by filtration and air-dried overnight to obtain Catalyst **C1-C4**.

The single crystals of each of the two complexes were obtained from a mixture of dichloromethane: hexane (1:3)

Catalyst C1

Selected IR data: (KBr, ν/cm^{-1}): 1587 ($\nu_{\text{C}=\text{N}}$). Anal. calcd for $\text{C}_{20}\text{H}_{18}\text{ClN}_3\text{OPd}$: C, 52.42; H, 3.96; N, 9.17 found C, 52.49; H, 3.87; N, 9.25. $^1\text{H-NMR}$ (400 MHz, CDCl_3) δ 9.36 (d, $J = 5.4$ Hz, 1H), 8.12 (s, 1H), 7.66 – 7.61 (m, 2H), 7.25 (s, 1H), 7.22 – 7.17 (m, 2H), 7.10 (s, 2H), 7.04 (d, $J = 8.4$ Hz, 2H), 6.87 (t, $J = 6.8$ Hz, 1H), 6.61 (d, $J = 9.4$ Hz, 1H), 4.81 (s, 2H), 3.89 (s, 3H). $^{13}\text{C-NMR}$ (101 MHz, CDCl_3) δ 173.69, 163.53, 161.37, 160.81, 152.81, 151.18, 150.86, 148.30, 133.62, 129.69, 122.50, 120.96, 117.91, 112.25, 61.52, 55.68. ESI-MS: 422.0542 [$\text{Pd}(\text{L}^1\text{-Cl})$]⁺ ion. Yield: 30.7 mg, 67%.

Catalyst C2

Catalyst **C2** was prepared by following the procedure described above for catalyst **C1**, instead of L^1H used L^2H .

Selected IR data: (KBr, ν/cm^{-1}): 1576 ($\nu_{\text{C}=\text{N}}$). Anal. calcd for $\text{C}_{21}\text{H}_{21}\text{ClN}_4\text{Pd}$: C, 53.52; H, 4.49; N, 11.89 found C, 53.41; H, 4.34; N, 11.76. $^1\text{H-NMR}$ (400 MHz, CDCl_3) δ 9.36 (d, $J = 7.5$ Hz, 1H), 7.95 (s, 1H), 7.60 (t, $J = 7.6$ Hz, 1H), 7.47 (d, $J = 2.5$

FULL PAPER

Hz, 1H), 7.10 (t, $J = 8.0, 5.2$ Hz, 3H), 7.05–7.03 (m, 2H), 6.83 (t, $J = 7.1$ Hz, 1H), 6.32 (d, $J = 11.1$ Hz, 1H), 4.81 (s, 2H), 3.10 (s, 6H) ESI-MS: 435.0786 $[\text{Pd}(\text{L}^2)\text{-Cl}]^+$ ion. Yield: 30.6 mg, 65%.

Catalyst C3

Catalyst **C3** was prepared by following the procedure described above for catalyst **C1**, instead of L¹H used L³H.

Selected IR data: (KBr, ν/cm^{-1}): 1588 ($\nu_{\text{C=N}}$). Anal. calcd for $\text{C}_{23}\text{H}_{25}\text{ClN}_4\text{Pd}$: C, 55.32; H, 5.05; N, 11.22 found C, 55.21; H, 5.22; N, 11.12. ¹H NMR (400 MHz, CDCl_3) δ 9.36 (d, $J = 7.5$ Hz, 1H), 7.95 (s, 1H), 7.60 (t, $J = 7.6$ Hz, 1H), 7.47 (d, $J = 2.5$ Hz, 1H), 7.16 (dd, $J = 8.0, 5.2$ Hz, 3H), 7.11 – 7.03 (m, 4H), 6.81 (t, $J = 6.9$ Hz, 1H), 6.32 (d, $J = 11.1$ Hz, 1H), 4.81 (s, 2H), 3.46 (d, $J = 7.1$ Hz, 4H), 1.22 (t, $J = 7.1$ Hz, 6H). ¹³C NMR (101 MHz, CDCl_3) δ 172.94, 160.02, 152.93, 151.15, 148.94, 148.82, 138.05, 130.51, 129.29, 126.84, 126.10, 123.89, 122.53, 119.53, 117.26, 107.25, 61.34, 44.78, 12.89. ESI-MS 463.1169 $[\text{Pd}(\text{L}^3)\text{-Cl}]^+$ ion. Yield: 34.5 mg 69%.

Catalyst C4

Catalyst **C4** was prepared by following the procedure described above for catalyst **C1**, instead of L¹H used L⁴H.

Selected IR data: (KBr, ν/cm^{-1}): 1576 ($\nu_{\text{C=N}}$) %. Anal. calcd for $\text{C}_{23}\text{H}_{23}\text{ClN}_4\text{OPd}$: C, 53.82; H, 4.52; N, 10.91 found C, 53.65; H, 4.71; N, 10.84. ¹H NMR (400 MHz, DMSO) δ 7.91 (dt, $J = 15.5, 7.6$ Hz, 1H), 7.76 – 7.54 (m, 4H), 7.52 – 7.44 (m, 2H), 7.38 (dd, $J = 15.5, 7.4$ Hz, 3H), 7.32 – 7.22 (m, 1H), 7.22 – 7.09 (m, 1H), 7.06 (t, $J = 7.6$ Hz, 1H), 7.01 – 6.86 (m, 1H), 5.42 (s, 2H) 3.46–3.34 (m, 4H), 1.80 (s, 4H). ESI-MS: 477.1173 $[\text{Pd}(\text{L}^4)\text{-Cl}]^+$ ion. Yield: 33.9 mg, 66%.

General procedure for direct arylation reaction

An oven-dried sealed tube (10 mL) was charged with 1-methyl-1H-imidazole (1.0 mmol) or 1,2-dimethyl-1H-imidazole 1.0 mmol, aryl halide (1.0 mmol), K_2CO_3 (2.0 mmol), pivalic acid (0.30 mmol), 0.05 mol% catalyst (one of **C1–C4**), and 2 mL of DMA. The flask was placed pre-heated oil bath at 130 °C under aerobic conditions. The mixture was cooled to room temperature and added 10 mL of water for quenched the reaction. This mixture was extracted with dichloromethane (3 x 10 mL). The combined extract was washed with water and dried over anhydrous Na_2SO_4 . The extracted solvent was removed under reduced pressure with a rotary evaporator to obtain the product. The crude products were purified by column chromatography on silica gel using dichloromethane/methanol

(20/1) as an eluent. ¹H NMR and ¹³C NMR data are depicted in supporting information Figures S42–S87.

Catalysed products

1-methyl-5-phenyl-1H-imidazole^[32] (**3aa**) Yellow solid. Yield 128.1 mg 81% (Catalyst **C1**), 140.8 mg 89% (Catalyst **C2**) 142.4 mg 90% (Catalyst **C3**), 136.0 mg 86% (Catalyst **C4**); ¹H-NMR (500 MHz, CDCl_3) δ 7.50 (s, 1H), 7.42 (t, $J = 7.3$ Hz, 2H), 7.36 (dd, $J = 13.9, 7.4$ Hz, 3H), 7.08 (s, 1H), 3.65 (s, 3H). ¹³C-NMR (126 MHz, CDCl_3) δ 139.07, 133.46, 129.84, 129.84, 128.74, 128.45, 128.10, 127.91, 32.54.

1-(4-(1-methyl-1H-imidazol-5-yl)phenyl)ethanone^[32] (**3ab**) Light yellow solid. Yield 174.2 mg 87% (Catalyst **C1**), 182.2 mg 91% (Catalyst **C2**) 184.2 mg 92% (Catalyst **C3**), 190.2 mg 95% (Catalyst **C4**); ¹H-NMR (500 MHz, CDCl_3) δ 8.00 (d, $J = 7.6$ Hz, 2H), 7.54 (s, 1H), 7.49 (d, $J = 7.6$ Hz, 2H), 7.19 (s, 1H), 3.71 (s, 3H), 2.61 (s, 3H). ¹³C-NMR (126 MHz, CDCl_3) δ 197.42, 140.13, 136.09, 134.44, 129.34, 128.86, 128.01, 32.90, 26.64.

4-(1-methyl-1H-imidazol-5-yl)benzaldehyde^[32] (**3ac**) Off-white solid. Yield 171.3 mg 92% (Catalyst **C1**), 165.7 mg 89% (Catalyst **C2**) 167.6 mg 90% (Catalyst **C3**), 173.1 mg 93% (Catalyst **C4**); ¹H-NMR (500 MHz, CDCl_3) δ 10.02 (s, 1H), 7.93 (d, $J = 7.6$ Hz, 2H), 7.56 (d, $J = 7.2$ Hz, 3H), 7.22 (s, 1H), 3.73 (s, 3H). ¹³C-NMR (126 MHz, CDCl_3) δ 191.54, 140.42, 135.80, 135.31, 132.28, 130.20, 129.78, 128.29, 32.98.

4-(1-methyl-1H-imidazol-5-yl)benzonitrile^[32] (**3ad**) Off-white solid. Yield 159.4 mg 87% (Catalyst **C1**), 170.4 mg 93% (Catalyst **C2**) 166.7 mg 91% (Catalyst **C3**), 175.7 mg 96% (Catalyst **C4**); ¹H-NMR (400 MHz, CDCl_3) δ 7.70 (d, $J = 8.6$ Hz, 2H), 7.55 (s, 1H), 7.50 (d, $J = 8.6$ Hz, 2H), 7.19 (d, $J = 0.6$ Hz, 1H), 3.70 (s, 3H). ¹³C-NMR (101 MHz, CDCl_3) δ 140.64, 134.51, 132.70, 131.77, 129.96, 128.41, 118.64, 111.36, 33.00.

1-methyl-5-(4-nitrophenyl)-1H-imidazole^[32] (**3ae**) Yellow solid. Yield 176.8 mg 87% (Catalyst **C1**), 180.8 mg 89% (Catalyst **C2**) 182.9 mg 90% (Catalyst **C3**), 191 mg 94% (Catalyst **C4**); ¹H-NMR (400 MHz, CDCl_3) δ 8.29 (d, $J = 8.8$ Hz, 2H), 7.58 (s, 2H), 7.55 (s, 1H), 7.26 (s, 1H), 3.75 (s, 3H). ¹³C-NMR (101 MHz, CDCl_3) δ 147.03, 140.94, 136.39, 131.46, 130.44, 128.36, 124.30, 33.12.

5-(4-chlorophenyl)-1-methyl-1H-imidazole^[32] (**3af**) Pale yellow solid. Yield 161.8 mg 84% (Catalyst **C1**), 156 mg 81% (Catalyst **C2**) 165.7 mg 86% (Catalyst **C3**), 154.1 mg 80% (Catalyst **C4**); ¹H-NMR (400 MHz, CDCl_3) δ 7.50 (s, 1H), 7.41 – 7.37 (m, 2H), 7.33 – 7.31 (m, 1H), 7.30 – 7.28 (m, 1H), 7.08

FULL PAPER

(s, 1H), 3.64 (s, 3H). ^{13}C -NMR (101 MHz, CDCl_3) δ 139.47, 134.07, 132.42, 129.75, 129.08, 128.36, 32.61.

5-(4-fluorophenyl)-1-methyl-1H-imidazole^[30] (3ag) Off-white solid. Yield 156.8 mg 89% (Catalyst **C1**), 160.3 mg 91% (Catalyst **C2**) 160.3 mg 91% (Catalyst **C3**), 165.6 mg 94% (Catalyst **C4**); ^1H -NMR (400 MHz, CDCl_3) δ 7.49 (s, 1H), 7.35 – 7.31 (m, 2H), 7.11 (t, J = 8.7 Hz, 2H), 7.04 (s, 1H), 3.61 (s, 3H). ^{13}C -NMR (101 MHz, CDCl_3) δ 163.85, 161.39, 139.13, 130.45, 128.20, 125.97, 115.99, 115.77, 32.49.

1-methyl-5-(p-tolyl)-1H-imidazole^[30] (3ah) Off-white solid. Yield 130.9 mg 76% (Catalyst **C1**), 134.3 mg 78% (Catalyst **C2**) 141.2 mg 82% (Catalyst **C3**), 148.1 mg 86% (Catalyst **C4**); ^1H -NMR (400 MHz, CDCl_3) δ 7.49 (s, 1H), 7.26 (d, J = 8.3 Hz, 2H), 7.22 (d, J = 8.1 Hz, 2H), 7.05 (s, 1H), 3.63 (s, 3H), 2.38 (s, 3H). ^{13}C -NMR (101 MHz, CDCl_3) δ 138.90, 137.92, 133.54, 129.50, 128.51, 127.76, 126.92, 32.55, 21.30.

5-(4-methoxyphenyl)-1-methyl-1H-imidazole^[32] (3ai) Yellow solid. Yield. 148.7 mg 79% (Catalyst **C1**), 152.5 mg 81% (Catalyst **C2**) 160 mg 85% (Catalyst **C3**), 156.2 mg 83% (Catalyst **C4**); ^1H -NMR (400 MHz, CDCl_3) δ 7.47 (s, 1H), 7.29 (d, J = 8.8 Hz, 2H), 7.01 (s, 1H), 6.95 (d, J = 8.8 Hz, 2H), 3.83 (s, 3H), 3.61 (s, 3H). ^{13}C -NMR (101 MHz, CDCl_3) δ 159.50, 138.67, 133.29, 130.02, 127.60, 122.26, 114.24, 55.43, 32.44.

5-(3-methoxyphenyl)-1-methyl-1H-imidazole^[32] (3aj) Light yellow solid. Yield 137.4 mg 73% (Catalyst **C1**), 141.1 mg 75% (Catalyst **C2**) 150.6 mg 80% (Catalyst **C3**), 156.2 mg 83% (Catalyst **C4**); ^1H -NMR (500 MHz, CDCl_3) δ 7.48 (s, 1H), 7.31 (t, J = 8.2 Hz, 1H), 7.06 (s, 1H), 6.93 (d, J = 7.6 Hz, 1H), 6.88 (d, J = 6.2 Hz, 2H), 3.80 (s, 3H), 3.64 (s, 3H). ^{13}C -NMR (126 MHz, CDCl_3) δ 159.73, 139.08, 133.32, 131.05, 129.78, 128.04, 120.84, 115.00, 114.31, 113.22, 55.33, 32.60.

3-(1-methyl-1H-imidazol-5-yl)pyridine^[30] (3ak) Light yellow liquid. Yield 120.9 mg 76% (Catalyst **C1**), 128.9 mg 81% (Catalyst **C2**) 127.3 mg 80% (Catalyst **C3**), 132.1 mg 85% (Catalyst **C4**); ^1H -NMR (400 MHz, CDCl_3) δ 7.93 – 7.88 (m, 2H), 7.63 (d, J = 7.5 Hz, 2H), 7.54 – 7.41 (m, 4H), 7.14 (s, 1H), 3.39 (s, 3H). ^{13}C -NMR (101 MHz, CDCl_3) δ 138.54, 133.72, 132.99, 131.24, 129.31, 129.15, 128.49, 127.34, 126.86, 126.28, 125.60, 125.32, 32.08.

1-methyl-5-(naphthalen-1-yl)-1H-imidazole^[32] (3al) Yellow liquid. Yield 158.3 mg 76% (Catalyst **C1**), 164.5 mg 79% (Catalyst **C2**) 168.7 mg 81% (Catalyst **C3**), 177 mg 85% (Catalyst **C4**); ^1H -NMR (400 MHz, CDCl_3) δ 7.92 – 7.88 (m, 2H), 7.63 (d, J = 8.5 Hz, 2H), 7.53 (d, J = 7.0 Hz, 2H), 7.46

(ddd, J = 15.0, 5.2, 1.4 Hz, 2H), 7.14 (s, 1H), 3.39 (s, 3H). ^{13}C -NMR (101 MHz, CDCl_3) δ 138.53, 133.73, 133.00, 131.25, 129.54, 129.32, 129.16, 128.49, 127.33, 126.86, 126.29, 125.60, 125.32, 32.08.

1,2-dimethyl-5-phenyl-1H-imidazole^[32] (4aa) Yellow liquid. Yield 142.9 mg 83% (Catalyst **C1**), 156.7 mg 91% (Catalyst **C2**) 160.2 mg 85% (Catalyst **C3**), 153.3 mg 89% (Catalyst **C4**); ^1H -NMR (400 MHz, CDCl_3) δ 7.45 – 7.37 (m, 2H), 7.34 (dd, J = 7.8, 1.8 Hz, 3H), 6.93 (s, 1H), 3.51 (s, 3H), 2.43 (s, 3H). ^{13}C -NMR (101 MHz, CDCl_3) δ 130.66, 128.77, 128.71, 127.74, 125.91, 31.43, 13.76.

1-(4-(1,2-dimethyl-1H-imidazol-5-yl)phenyl)ethanone^[32] (4ab) Light yellow solid. Yield 192.8 mg 90% (Catalyst **C1**), 201.4 mg 94% (Catalyst **C2**) 194.9 mg 91% (Catalyst **C3**), 199.3 mg 93% (Catalyst **C4**); ^1H -NMR (400 MHz, CDCl_3) δ 7.98 (d, J = 8.5 Hz, 2H), 7.43 (d, J = 8.5 Hz, 2H), 7.03 (s, 1H), 3.55 (s, 3H), 2.59 (s, 3H), 2.43 (s, 3H). ^{13}C -NMR (101 MHz, CDCl_3) δ 197.52, 147.31, 135.84, 135.25, 132.65, 128.90, 128.04, 127.36, 31.77, 26.72, 13.87.

4-(1,2-dimethyl-1H-imidazol-5-yl)benzaldehyde^[32] (4ac) Off-white solid. Yield 176.2 mg 88% (Catalyst **C1**), 182.2 mg 91% (Catalyst **C2**) 186.2 mg 93% (Catalyst **C3**), 190.2 mg 95% (Catalyst **C4**); ^1H NMR (400 MHz, CDCl_3) δ 10.01 (s, 1H), 7.91 (d, J = 8.7 Hz, 2H), 7.51 (d, J = 8.4 Hz, 2H), 7.07 (s, 1H), 3.58 (s, 3H), 2.45 (s, 3H). ^{13}C NMR (101 MHz, CDCl_3) δ 191.66, 136.60, 135.12, 130.27, 128.35, 127.81, 31.84, 13.86.

4-(1,2-dimethyl-1H-imidazol-5-yl)benzonitrile^[32] (4ad) Light yellow solid. Yield 177.5 mg 90% (Catalyst **C1**), 183.4 mg 93% (Catalyst **C2**) 185.4 mg 94% (Catalyst **C3**), 189.3 mg 96% (Catalyst **C4**); ^1H -NMR (500 MHz, CDCl_3) δ 7.72 (d, J = 7.4 Hz, 2H), 7.49 (d, J = 7.5 Hz, 2H), 7.08 (s, 1H), 3.59 (s, 3H), 2.48 (s, 3H). ^{13}C NMR (101 MHz, CDCl_3) δ 135.11, 132.56, 128.34, 127.86, 118.63, 110.92, 31.68, 13.74.

1,2-dimethyl-5-(4-nitrophenyl)-1H-imidazole^[32] (4ae) Off-white solid. Yield 191.2 mg 88% (Catalyst **C1**), 197.7 mg 91% (Catalyst **C2**) 204.2 mg 94% (Catalyst **C3**), 208.5 mg 96% (Catalyst **C4**); ^1H -NMR (400 MHz, CDCl_3) δ 8.26 (d, J = 8.8 Hz, 2H), 7.50 (d, J = 8.8 Hz, 2H), 7.09 (s, 1H), 3.59 (s, 3H), 2.46 (s, 3H). ^{13}C -NMR (101 MHz, CDCl_3) δ 148.49, 147.40, 134.21, 132.26, 131.29, 129.96, 127.50, 122.86, 122.38, 31.63, 13.84.

5-(4-chlorophenyl)-1,2-dimethyl-1H-imidazole^[32] (4af) Light yellow solid. Yield 161.2 mg 78% (Catalyst **C1**), 167.4 mg 81% (Catalyst **C2**) 169.5 mg 82% (Catalyst **C3**), 173.6 mg 84% (Catalyst **C4**); ^1H -NMR (400 MHz, CDCl_3) δ 7.37 (d, J = 8.5 Hz,

FULL PAPER

2H), 7.26 (d, $J = 8.6$ Hz, 2H), 6.92 (s, 1H), 3.48 (s, 3H), 2.42 (s, 3H). $^{13}\text{C-NMR}$ (101 MHz, CDCl_3) δ 146.42, 133.72, 132.47, 129.85, 129.08, 126.35, 31.40, 13.84.

5-(4-fluorophenyl)-1,2-dimethyl-1H-imidazole^[30] (4ag) Off-white solid. Yield 144.6 mg 76% (Catalyst **C1**), 142.7 mg 75% (Catalyst **C2**) 152.2 mg 80% (Catalyst **C3**), 157.9 mg 83% (Catalyst **C4**); $^1\text{H-NMR}$ (500 MHz, CDCl_3) δ 7.88 (d, $J = 7.5$ Hz, 2H), 7.64 (d, $J = 7.5$ Hz, 2H), 7.24 (s, 1H), 3.75 (s, 3H), 2.64 (s, 3H). $^{13}\text{C-NMR}$ (101 MHz, CDCl_3) δ 148.49, 147.40, 134.21, 132.26, 131.30, 129.96, 127.50, 122.68, 122.26, 31.6, 13.84.

5-(4-methoxyphenyl)-1,2-dimethyl-1H-imidazole^[32] (4ah) Off-white solid. Yield 157.8 mg 78% (Catalyst **C1**), 163.8 mg 81% (Catalyst **C2**) 165.8 mg 82% (Catalyst **C3**), 169.9 mg 84% (Catalyst **C4**); $^1\text{H-NMR}$ (400 MHz, CDCl_3) δ 7.25 (d, $J = 8.8$ Hz, 2H), 6.94 (d, $J = 8.8$ Hz, 2H), 6.87 (s, 1H), 3.83 (s, 3H), 3.46 (s, 3H), 2.42 (s, 3H). $^{13}\text{C-NMR}$ (126 MHz, CDCl_3) δ 170.68, 159.28, 133.24, 130.04, 125.13, 122.94, 114.10, 55.28, 31.07, 13.56.

1,2-dimethyl-5-(p-tolyl)-1H-imidazole^[30] (4ai) Light yellow solid. Yield 149 mg 80% (Catalyst **C1**), 154.6 mg 83% (Catalyst **C2**) 156.4 mg 84% (Catalyst **C3**), 162 mg 87% (Catalyst **C4**); $^1\text{H-NMR}$ (400 MHz, CDCl_3) δ 7.20 (s, 4H), 6.88 (s, 1H), 3.46 (s, 3H), 2.40 (s, 3H), 2.35 (s, 3H). $^{13}\text{C-NMR}$ (101 MHz, CDCl_3) δ 145.78, 137.66, 133.64, 129.58, 128.75, 127.60, 125.52, 31.34, 21.28, 13.82.

5-(3-methoxyphenyl)-1,2-dimethyl-1H-imidazole^[30] (4aj) Off-white solid. Yield 153.7 mg 76% (Catalyst **C1**), 151.7 mg 75% (Catalyst **C2**) 161.8 mg 80% (Catalyst **C3**), 167.9 mg 83% (Catalyst **C4**); $^1\text{H-NMR}$ (500 MHz, CDCl_3) δ 7.33 (t, $J = 7.8$ Hz, 1H), 6.96 – 6.91 (m, 2H), 6.89 (d, $J = 6.2$ Hz, 2H), 3.82 (s, 3H), 3.52 (s, 3H), 2.43 (s, 3H). $^{13}\text{C-NMR}$ (126 MHz, CDCl_3) δ 159.74, 146.00, 133.41, 131.86, 129.67, 125.89, 120.95, 114.38, 113.02, 55.27, 31.33, 13.62.

3-(1,2-dimethyl-1H-imidazol-5-yl)pyridine^[30] (3ak) Light yellow liquid. Yield 135.1 mg 78% (Catalyst **C1**), 140.3 mg 81% (Catalyst **C2**) 143.8 mg 83% (Catalyst **C3**), 148.9 mg 86% (Catalyst **C4**); $^1\text{H-NMR}$ (400 MHz, CDCl_3) δ 8.60 (d, $J = 3.0$ Hz, 1H), 8.55 (dd, $J = 4.9, 1.7$ Hz, 1H), 7.66 – 7.62 (m, 1H), 7.33 (dd, $J = 7.5, 5.3$ Hz, 1H), 6.98 (s, 1H), 3.51 (s, 3H), 2.43 (s, 3H). $^{13}\text{C-NMR}$ (101 MHz, CDCl_3) δ 149.25, 148.81, 147.02, 135.76, 130.14, 127.03, 126.75, 123.61, 31.46, 13.75.

1,2-dimethyl-5-(naphthalen-1-yl)-1H-imidazole^[32] (3al) Light yellow liquid. Yield 182.2 mg 80% (Catalyst **C1**), 186.7 mg 83% (Catalyst **C2**) 186.7 mg 84% (Catalyst **C3**), 193.3 mg 87%

(Catalyst **C4**); $^1\text{H-NMR}$ (400 MHz, CDCl_3) δ 7.88 (d, $J = 7.7$ Hz, 2H), 7.65 (d, $J = 8.2$ Hz, 1H), 7.53 – 7.36 (m, 4H), 6.99 (s, 1H), 3.23 (s, 3H), 2.48 (s, 3H). $^{13}\text{C-NMR}$ (101 MHz, CDCl_3) δ 145.59, 133.73, 133.00, 131.19, 129.14, 128.46, 128.08, 126.76, 126.21, 125.69, 125.34, 31.08, 13.74.

Typical procedure for Mizoroki-Heck reactions

An oven-dried sealed tube (10 mL) was charged with 0.001 mol% of pallacycles(II) catalyst, 1 mmol of aryl halide, 1.2 mmol of methyl acrylate/tert-butyl acrylate/styrene, 2 mmol of Et_3N and 2.0 mL of NMP. The reaction flask was heated at 140 °C for 8 h in an oil bath. The reaction was tested by TLC, the reaction mixture was cooled to ambient temperature, H_2O (5 mL) was added and the organic layer was extracted with dichloromethane (3x10 mL). The combined organic layers were dried with sodium sulfate and concentrated. The crude product was purified by column chromatography (ethyl acetate-hexane). ^1H NMR and ^{13}C NMR data are depicted in supporting information Figures S88-S156.

Methyl cinnamate (7aa) White solid. Yield 142.7 mg 88% (Catalyst **C1**), 147.6 mg 91% (Catalyst **C2**); $^1\text{H-NMR}$ (400 MHz, CDCl_3) δ 7.69 (d, $J = 16.0$ Hz, 1H), 7.50 (dd, $J = 6.5, 3.0$ Hz, 2H), 7.38 – 7.35 (m, 3H), 6.43 (d, $J = 16.1$ Hz, 1H), 3.79 (s, 3H). $^{13}\text{C-NMR}$ (101 MHz, CDCl_3) δ 167.50 (s), 144.97, 134.46, 130.41, 130.19, 128.58, 117.87, 51.77.

(E)-methyl-3-(4-hydroxyphenyl)acrylate (7ab) White solid. Yield 128.3 mg 72% (Catalyst **C1**), 133.6 mg 75% (Catalyst **C2**); $^1\text{H-NMR}$ (400 MHz, CDCl_3) δ 7.62 (d, $J = 16.0$ Hz, 1H), 7.41 (d, $J = 8.5$ Hz, 2H), 6.83 (d, $J = 8.7$ Hz, 2H), 6.28 (d, $J = 15.9$ Hz, 1H), 3.78 (s, 3H). ^{13}C NMR (101 MHz, CDCl_3) δ 168.29, 158.05, 144.88, 130.19, 127.26, 116.06, 115.27, 51.91.

(E)-methyl 3-(4-formylphenyl)acrylate (7ac) White solid. Yield 144.5 mg 76% (Catalyst **C1**), 152.2 mg 80% (Catalyst **C2**); $^1\text{H-NMR}$ (400 MHz, CDCl_3) δ 9.53 (s, 1H), 7.41 (d, $J = 8.1$ Hz, 2H), 7.23 – 7.15 (m, 3H), 6.06 (d, $J = 15.9$ Hz, 1H), 3.33 (s, 3H). ^{13}C NMR (101 MHz, CDCl_3) δ 191.57, 166.89, 143.19, 140.10, 137.26, 130.26, 128.56, 121.08, 52.00.

(E)-methyl 3-(4-acetylphenyl)acrylate (7ad) White solid. Yield 179.7 mg 88% (Catalyst **C1**), 185.8 mg 91% (Catalyst **C2**); $^1\text{H-NMR}$ (400 MHz, CDCl_3) δ 7.94 (d, $J = 8.4$ Hz, 2H), 7.68 (d, $J = 16.1$ Hz, 1H), 7.58 (d, $J = 8.3$ Hz, 2H), 6.50 (d, $J = 16.1$ Hz, 1H), 3.80 (s, 3H), 2.59 (s, 3H). $^{13}\text{C-NMR}$ (101 MHz, CDCl_3) δ 197.48, 167.05, 143.40, 138.77, 138.09, 128.95, 128.24, 120.40, 52.01, 26.79.

FULL PAPER

(E)-methyl 3-(p-tolyl)acrylate (7ae) White solid. Yield 137.4 mg 78% (Catalyst **C1**), 139.2 mg 79% (Catalyst **C2**); ¹H-NMR (400 MHz, CDCl₃) δ 7.65 (d, *J* = 16.4 Hz, 1H), 7.40 (d, *J* = 8.2 Hz, 2H), 7.17 (d, *J* = 8.0 Hz, 2H), 6.37 (d, *J* = 16.0 Hz, 1H), 3.77 (s, 3H), 2.35 (s, 3H). ¹³C NMR (101 MHz, CDCl₃) δ 167.76, 144.98, 140.82, 131.7, 129.72, 128.16, 116.75, 51.75, 21.56.

(E)-methyl 3-(4-nitrophenyl)acrylate (7af) Slightly yellow solid. Yield 180.3 mg 87% (Catalyst **C1**), 184.4 mg 99% (Catalyst **C2**); ¹H-NMR (400 MHz, CDCl₃) δ 8.23 (d, *J* = 8.8 Hz, 2H), 7.70 (d, *J* = 16.1 Hz, 1H), 7.65 (d, *J* = 8.7 Hz, 2H), 6.54 (d, *J* = 16.1 Hz, 1H), 3.82 (s, 3H). ¹³C-NMR (101 MHz, CDCl₃) δ 166.58, 142.00, 140.55, 128.74, 124.27, 122.17, 52.18.

(E)-methyl 3-(2-nitrophenyl)acrylate (7ag) Slightly yellow solid. Yield 145 mg 70% (Catalyst **C1**), 155.4 mg 75% (Catalyst **C2**); ¹H NMR (400 MHz, CDCl₃) δ 8.10 (d, *J* = 15.8 Hz, 1H), 8.03 (d, *J* = 8.9 Hz, 1H), 7.65 – 7.60 (m, 2H), 7.55 – 7.51 (m, 1H), 6.35 (d, *J* = 15.8 Hz, 1H), 3.82 (s, 3H). ¹³C-NMR (101 MHz, CDCl₃) δ 166.32, 140.26, 133.63, 130.66, 130.40, 129.22, 125.01, 122.95, 52.12.

(E)-methyl 3-(3-nitrophenyl)acrylate (7ah) Slightly yellow solid. Yield 167.8 mg 81% (Catalyst **C1**), 176.1 mg 85% (Catalyst **C2**); ¹H-NMR (500 MHz, CDCl₃) δ 8.36 (s, 1H), 8.22 (d, *J* = 8.1 Hz, 1H), 7.83 (d, *J* = 7.6 Hz, 1H), 7.70 (s, 1H), 7.59 (t, *J* = 8.0 Hz, 1H), 6.56 (d, *J* = 16.0 Hz, 1H), 3.83 (s, 3H). ¹³C-NMR (126 MHz, CDCl₃) δ 166.68, 148.67, 141.94, 136.11, 133.62, 129.98, 124.53, 122.42, 121.17, 115.00, 51.99.

(E)-methyl 3-(4-cyanophenyl)acrylate (7ai) White solid. Yield 162.9 mg 87% (Catalyst **C1**), 166.6 mg 89% (Catalyst **C2**); ¹H-NMR (500 MHz, CDCl₃) δ 7.72 – 7.66 (m, 3H), 7.62 (d, *J* = 7.8 Hz, 2H), 6.54 (d, *J* = 16.0 Hz, 1H), 3.84 (s, 3H). ¹³C-NMR (126 MHz, CDCl₃) δ 166.57 (s), 142.41, 138.66, 132.66, 128.40, 121.40, 118.33, 113.44, 52.02.

(E)-methyl 3-(4-fluorophenyl)acrylate (7aj) Yellow solid. Yield 151.3 mg 84% (Catalyst **C1**), 154.9 mg 86% (Catalyst **C2**); ¹H-NMR (500 MHz, CDCl₃) δ 7.68 (d, *J* = 16.0 Hz, 1H), 7.57 – 7.52 (m, 2H), 7.10 (t, *J* = 8.4 Hz, 2H), 6.39 (d, *J* = 16.0 Hz, 1H), 3.83 (s, 3H). ¹³C-NMR (126 MHz, CDCl₃) δ 167.29, 164.92, 143.56, 129.97, 117.59, 116.07, 115.00, 51.72.

(E)-methyl 3-(4-chlorophenyl)acrylate (7ak) White solid. Yield 157.3 mg 80% (Catalyst **C1**), 163.2 mg 83% (Catalyst **C2**); ¹H-NMR (500 MHz, CDCl₃) δ 7.61 (d, *J* = 16.0 Hz, 1H), 7.43 (d, *J* = 8.4 Hz, 2H), 7.33 (d, *J* = 8.4 Hz, 2H), 6.38 (d, *J* =

16.0 Hz, 1H), 3.78 (s, 3H). ¹³C-NMR (126 MHz, CDCl₃) δ 167.17, 143.41, 136.22, 132.88, 129.19, 118.40, 51.79.

(E)-methyl 3-(naphthalen-1-yl)acrylate (7al) Light yellow oil. Yield 142.2 mg 67% (Catalyst **C1**), 150.7 mg 71% (Catalyst **C2**); ¹H-NMR (500 MHz, CDCl₃) δ 8.57 (d, *J* = 15.8 Hz, 1H), 8.23 (d, *J* = 8.4 Hz, 1H), 7.92 (t, *J* = 9.0 Hz, 2H), 7.79 (d, *J* = 7.2 Hz, 1H), 7.60 (d, *J* = 8.2 Hz, 1H), 7.59 – 7.54 (m, 1H), 7.52 (t, *J* = 7.7 Hz, 1H), 6.56 (d, *J* = 15.8 Hz, 1H), 3.89 (s, 3H).

tert-butyl cinnamate^{9a} (8aa) Colorless oil. Yield 181.8 mg 89% (Catalyst **C1**), 185.9 mg 91% (Catalyst **C2**); ¹H-NMR (400 MHz, CDCl₃) δ 7.57 (d, *J* = 16.0 Hz, 1H), 7.48 (dd, *J* = 6.6, 3.1 Hz, 2H), 7.34 (dd, *J* = 5.0, 1.9 Hz, 3H), 6.35 (d, *J* = 16.0 Hz, 1H), 1.52 (s, 9H). ¹³C-NMR (101 MHz, CDCl₃) δ 166.44, 143.64, 134.77, 130.08, 128.94, 128.07, 120.27, 80.60, 28.36.

(E)-tert-butyl 3-(4-hydroxyphenyl)acrylate (8ab) White solid. Yield 178.4 mg 81% (Catalyst **C1**), 174 mg 79% (Catalyst **C2**); ¹H-NMR (400 MHz, CDCl₃) δ 7.51 (d, *J* = 16.1 Hz, 1H), 7.34 (d, *J* = 9.0 Hz, 2H), 6.85 (d, *J* = 8.9 Hz, 2H), 6.19 (d, *J* = 16.0 Hz, 1H), 1.52 (s, 9H). ¹³C-NMR (101 MHz, CDCl₃) δ 168.08, 158.57, 144.41, 130.14, 126.87, 116.94, 116.15, 81.24, 28.42.

(E)-tert-butyl 3-(4-formylphenyl)acrylate^{9a} (8ac) Colorless oil. Yield 188.1 mg 81% (Catalyst **C1**), 197.4 mg 85% (Catalyst **C2**); ¹H-NMR (400 MHz, CDCl₃) δ 10.01 (s, 1H), 7.87 (d, *J* = 8.2 Hz, 2H), 7.64 (d, *J* = 8.2 Hz, 2H), 7.59 (d, *J* = 16.0 Hz, 1H), 6.47 (d, *J* = 16.0 Hz, 1H), 1.53 (s, 9H). ¹³C-NMR (101 MHz, CDCl₃) δ 191.59, 165.72, 141.89, 140.51, 137.04, 130.22, 128.46, 123.53, 81.16, 28.26.

(E)-tert-butyl 3-(4-acetylphenyl)acrylate^{9a} (8ad) Colorless oil. Yield 219.2 mg 89% (Catalyst **C1**), 229 mg 93% (Catalyst **C2**); ¹H-NMR (500 MHz, CDCl₃) δ 7.93 (d, *J* = 8.3 Hz, 2H), 7.59 – 7.55 (m, 3H), 6.43 (d, *J* = 16.1 Hz, 1H), 2.59 (s, 3H), 1.51 (s, 9H). ¹³C NMR (101 MHz, CDCl₃) δ 197.54, 165.89, 142.06, 139.15, 137.84, 128.91, 128.10, 122.85, 81.00, 28.38.

(E)-tert-butyl 3-(p-tolyl)acrylate^{9a} (8ae) Colorless oil. Yield 172.4 mg 79% (Catalyst **C1**), 176.8 mg 81% (Catalyst **C2**); ¹H-NMR (400 MHz, CDCl₃) δ 7.54 (d, *J* = 16.0 Hz, 1H), 7.38 (d, *J* = 8.1 Hz, 2H), 7.15 (d, *J* = 8.0 Hz, 2H), 6.30 (d, *J* = 16.0 Hz, 1H), 2.34 (s, 3H), 1.51 (s, 9H). ¹³C-NMR (101 MHz, CDCl₃) δ 166.66, 143.64, 140.40, 131.98, 129.62, 128.04, 119.15, 80.46, 28.30, 21.53.

(E)-tert-butyl 3-(4-nitrophenyl)acrylate^{9a} (8af) Yellow solid. Yield 219.4 mg 88% (Catalyst **C1**), 224.3 mg 90% (Catalyst **C2**); ¹H-NMR (400 MHz, CDCl₃) δ 8.22 (d, *J* = 9.1 Hz, 2H), 7.64

FULL PAPER

(d, $J = 8.8$ Hz, 2H), 7.59 (d, $J = 16.0$ Hz, 1H), 6.48 (d, $J = 16.1$ Hz, 1H), 1.57 (s, 9H). $^{13}\text{C-NMR}$ (101 MHz, CDCl_3) δ 165.38, 140.95, 140.67, 128.58, 124.63, 124.22, 81.44, 28.21.

(E)-tert-butyl 3-(2-nitrophenyl)acrylate (8ag) Yellow solid. Yield 199.4 mg 80% (Catalyst **C1**), 211.8 mg 85% (Catalyst **C2**); $^1\text{H-NMR}$ (400 MHz, CDCl_3) δ 8.01 – 7.95 (m, 2H), 7.61 (d, $J = 4.0$ Hz, 2H), 7.52 – 7.47 (m, 1H), 6.27 (d, $J = 15.8$ Hz, 1H), 1.51 (s, 9H). $^{13}\text{C-NMR}$ (101 MHz, CDCl_3) δ 165.15, 138.79, 133.50, 130.86, 130.12, 129.19, 125.36, 124.94, 81.28, 28.20.

(E)-tert-butyl 3-(naphthalen-1-yl)acrylate^[9a] Yellow liquid. Yield 165.3 mg 65% (Catalyst **C1**), 178 mg 70% (Catalyst **C2**); $^1\text{H-NMR}$ (400 MHz, CDCl_3) δ 8.22 (d, $J = 15.6$ Hz, 2H), 8.18 (d, $J = 8.4$ Hz, 1H), 7.86 (d, $J = 8.4$ Hz, 2H), 7.71 (d, $J = 8.2$ Hz, 1H), 7.56 (m, 3H), 6.45 (d, $J = 15.6$ Hz, 1H), 1.57 (s, 9H). $^{13}\text{C-NMR}$ (101 MHz, CDCl_3) δ 166.34, 140.78, 140.56, 133.72, 132.13, 131.50, 130.27, 128.76, 126.82, 126.18, 125.54, 125.00, 123.71, 122.90, 81.38, 28.43.

(E)-1,2-diphenylethene^[9a] (9aa) White solids. Yield 160.4 mg 89% (Catalyst **C1**), 164 mg 91% (Catalyst **C2**); $^1\text{H-NMR}$ (400 MHz, CDCl_3) δ 7.53 (s, 2H), 7.51 (s, 2H), 7.36 (t, $J = 7.6$ Hz, 4H), 7.29 – 7.24 (m, 2H), 7.12 (s, 2H). $^{13}\text{C-NMR}$ (101 MHz, CDCl_3) δ 137.49, 128.86, 127.8, 126.68.

(E)-4-styrylphenol (9ab) White solids. Yield 137.4 mg 70% (Catalyst **C1**), 147.2 mg 75% (Catalyst **C2**); $^1\text{H-NMR}$ (400 MHz, CDCl_3) δ 7.47 (d, $J = 9.3$ Hz, 2H), 7.39 (d, $J = 8.9$ Hz, 2H), 7.33 (t, $J = 7.9$ Hz, 2H), 7.24 – 7.19 (m, 1H), 7.07 – 6.92 (m, 2H), 6.81 (d, $J = 8.9$ Hz, 2H). $^{13}\text{C-NMR}$ (101 MHz, CDCl_3) δ 155.53, 137.78, 130.45, 128.88, 128.33, 128.14, 127.47, 126.81, 126.47, 115.83.

(E)-4-styrylbenzaldehyde^[47] (9ac) White solids. Yield 170.8 mg 82% (Catalyst **C1**), 181.2 mg 87% (Catalyst **C2**); $^1\text{H-NMR}$ (500 MHz, CDCl_3) δ 10.02 (s, 1H), 7.90 (d, $J = 8.0$ Hz, 2H), 7.68 (d, $J = 8.0$ Hz, 2H), 7.58 (d, $J = 7.8$ Hz, 2H), 7.42 (t, $J = 7.5$ Hz, 2H), 7.34 (t, $J = 7.1$ Hz, 1H), 7.31 – 7.26 (m, 1H), 7.17 (d, $J = 16.3$ Hz, 1H). $^{13}\text{C-NMR}$ (126 MHz, CDCl_3) δ 191.57, 143.42, 136.56, 135.35, 132.20, 130.23, 128.83, 128.50, 127.34, 126.91.

(E)-1-(4-styrylphenyl)ethanone^[9a] (9ad) White solids. Yield 202.3 mg 91% (Catalyst **C1**), 211.2 mg 95% (Catalyst **C2**); $^1\text{H-NMR}$ (400 MHz, CDCl_3) δ 7.94 (d, $J = 8.4$ Hz, 2H), 7.57 (d, $J = 8.3$ Hz, 2H), 7.52 (d, $J = 7.2$ Hz, 2H), 7.37 (t, $J = 7.5$ Hz, 2H), 7.29 (d, $J = 7.3$ Hz, 1H), 7.21 (d, $J = 16.3$ Hz, 1H), 7.11 (d, $J = 16.3$ Hz, 1H), 2.59 (s, 3H). $^{13}\text{C-NMR}$ (101 MHz, CDCl_3) δ

197.61, 142.09, 136.78, 136.02, 128.97, 126.91, 126.60, 26.69.

(E)-1-methoxy-4-styrylbenzene^[9a] (9ae) White solids. Yield 151.4 mg 72% (Catalyst **C1**), 155.6 mg 74% (Catalyst **C2**); $^1\text{H-NMR}$ (400 MHz, CDCl_3) δ 7.46 (dd, $J = 13.3, 8.0$ Hz, 4H), 7.34 (t, $J = 7.6$ Hz, 2H), 7.22 (t, $J = 7.9$ Hz, 1H), 7.06 (d, $J = 16.3$ Hz, 1H), 6.97 (d, $J = 16.3$ Hz, 1H), 6.89 (d, $J = 8.8$ Hz, 2H), 3.82 (s, 3H). $^{13}\text{C-NMR}$ (101 MHz, CDCl_3) δ 159.37, 137.72, 130.22, 128.73, 128.28, 127.79, 127.30, 126.69, 126.33, 114.21, 55.42.

(E)-1-nitro-4-styrylbenzene^[47] (9af) Off-white solids. Yield 184.7 mg 82% (Catalyst **C1**), 193.7 mg 86% (Catalyst **C2**); $^1\text{H-NMR}$ (500 MHz, CDCl_3) δ 7.94 (d, $J = 8.2$ Hz, 1H), 7.75 (d, $J = 7.9$ Hz, 1H), 7.62 – 7.55 (m, 2H), 7.53 (d, $J = 7.7$ Hz, 2H), 7.37 (t, $J = 7.4$ Hz, 3H), 7.31 (t, $J = 7.2$ Hz, 1H), 7.07 (d, $J = 16.1$ Hz, 1H). $^{13}\text{C-NMR}$ (126 MHz, CDCl_3) δ 148.03, 136.51, 133.89, 133.10, 130.04, 128.84, 128.64, 128.19, 127.98, 127.11, 124.79, 123.52.

(E)-1-nitro-2-styrylbenzene (9ag) Off-white solids. Yield 182.4 mg 81% (Catalyst **C1**), 193.7 mg 86% (Catalyst **C2**); $^1\text{H-NMR}$ (500 MHz, CDCl_3) δ 8.17 (d, $J = 8.3$ Hz, 2H), 7.59 (d, $J = 8.3$ Hz, 2H), 7.51 (d, $J = 7.8$ Hz, 2H), 7.35 (t, $J = 7.5$ Hz, 2H), 7.29 (t, $J = 7.2$ Hz, 1H), 7.21 (s, 2H), 7.10 (d, $J = 16.3$ Hz, 1H). $^{13}\text{C-NMR}$ (101 MHz, CDCl_3) δ 148.08, 136.57, 133.95, 133.21, 133.11, 128.92, 128.72, 128.26, 128.06, 127.19, 124.88, 123.59.

(E)-1-nitro-3-styrylbenzene (9ah) Off-white solids. Yield 159.9 mg 71% (Catalyst **C1**), 168.9 mg 75% (Catalyst **C2**); $^1\text{H-NMR}$ (400 MHz, CDCl_3) δ 8.36 (t, $J = 1.9$ Hz, 1H), 8.09 (ddd, $J = 8.1, 2.2, 0.8$ Hz, 1H), 7.79 (d, $J = 7.8$ Hz, 1H), 7.56 – 7.51 (m, 3H), 7.39 (t, $J = 7.5$ Hz, 2H), 7.31 (t, $J = 7.3$ Hz, 1H), 7.23 (d, $J = 14.5$ Hz, 1H), 7.12 (d, $J = 16.3$ Hz, 1H). $^{13}\text{C-NMR}$ (126 MHz, CDCl_3) δ 148.57, 136.68, 133.01, 132.65, 130.85, 128.80, 128.22, 126.68, 124.92, 123.52, 115.00.

(E)-4-styrylbenzonitrile^[47] (9ai) White solids. Yield 176.5 mg 86% (Catalyst **C1**), 182.7 mg 89% (Catalyst **C2**); $^1\text{H-NMR}$ (500 MHz, CDCl_3) δ 7.66 (d, $J = 8.3$ Hz, 2H), 7.61 (d, $J = 8.1$ Hz, 2H), 7.56 (d, $J = 7.7$ Hz, 2H), 7.42 (t, $J = 7.5$ Hz, 2H), 7.35 (t, $J = 7.3$ Hz, 1H), 7.29 – 7.23 (m, 1H), 7.12 (d, $J = 16.3$ Hz, 1H). $^{13}\text{C-NMR}$ (126 MHz, CDCl_3) δ 141.86, 136.31, 132.51, 128.88, 126.93, 119.03, 115.00, 110.61.

(E)-1-fluoro-4-styrylbenzene (9aj) White solids. Yield 156.6 mg 79% (Catalyst **C1**), 160.6 mg 81% (Catalyst **C2**); $^1\text{H-NMR}$ (500 MHz, CDCl_3) δ 7.54 (d, $J = 7.9$ Hz, 3H), 7.47 (d, $J =$

FULL PAPER

8.3 Hz, 3H), 7.40 (t, $J = 7.5$ Hz, 3H), 7.36 (d, $J = 8.3$ Hz, 3H), 7.30 (dd, $J = 13.4, 6.5$ Hz, 2H), 7.10 (d, $J = 4.2$ Hz, 3H). ^{13}C -NMR (126 MHz, CDCl_3) δ 137.01, 135.88, 133.19, 129.35, 128.81, 127.89, 127.68, 127.39, 126.57.

(E)-1-chloro-4-styrylbenzene (9ak) White solids. Yield 163.2 mg 76% (Catalyst **C1**), 171.8 mg 80% (Catalyst **C2**); ^1H -NMR (400 MHz, CDCl_3) δ 7.50 (d, $J = 7.1$ Hz, 2H), 7.43 (d, $J = 8.5$ Hz, 2H), 7.37 (d, $J = 7.2$ Hz, 1H), 7.35 – 7.30 (m, 3H), 7.30 – 7.25 (m, 1H), 7.06 (d, $J = 2.9$ Hz, 2H). ^{13}C NMR (126 MHz, CDCl_3) δ 137.07, 135.94, 133.26, 129.41, 128.92, 128.81, 127.95, 127.74, 127.45, 126.64.

(E)-1-styrylnaphthalene (9al) White solids. Yield 154.3 mg 67% (Catalyst **C1**), 161.2 mg 70% (Catalyst **C2**); ^1H -NMR (500 MHz, CDCl_3) δ 8.47 (d, $J = 8.0$ Hz, 1H), 8.11 (dd, $J = 20.0, 11.9$ Hz, 2H), 8.02 (d, $J = 8.1$ Hz, 1H), 7.96 (d, $J = 7.1$ Hz, 1H), 7.82 (d, $J = 7.4$ Hz, 2H), 7.72 (dt, $J = 15.0, 8.5$ Hz, 3H), 7.63 (t, $J = 7.4$ Hz, 2H), 7.54 (t, $J = 7.2$ Hz, 1H), 7.38 (d, $J = 16.0$ Hz, 1H). ^{13}C NMR (126 MHz, CDCl_3) δ 137.91, 135.28, 134.04, 132.03, 131.72, 129.03, 128.92, 128.34, 128.05, 127.01, 126.38, 126.37, 126.11, 124.08, 123.94.

(E)-methyl 3-(pyridin-3-yl)acrylate (10aa) Yellow solid. Yield 122.4 mg 75% (Catalyst **C1**), 132.2 mg 81% (Catalyst **C2**); ^1H -NMR (500 MHz, CDCl_3) δ 8.74 (s, 1H), 8.60 (d, $J = 4.6$ Hz, 1H), 7.83 (d, $J = 7.8$ Hz, 1H), 7.68 (d, $J = 16.1$ Hz, 1H), 7.39 – 7.30 (m, 1H), 6.51 (d, $J = 16.1$ Hz, 1H), 3.82 (s, 3H). ^{13}C -NMR (126 MHz, CDCl_3) δ 166.71, 150.93 (s), 149.69 (s), 141.12 (s), 134.21, 130.14, 123.73, 120.00, 115.00, 51.88.

(E)-tert-butyl 3-(pyridin-3-yl)acrylate^[9a] (10ab) Colorless oil. Yield 158 mg 77% (Catalyst **C1**), 162.2 mg 79% (Catalyst **C2**); ^1H -NMR (400 MHz, CDCl_3) δ 8.67 (s, 1H), 8.52 (d, $J = 4.8$ Hz, 1H), 7.76 (d, $J = 9.9$ Hz, 1H), 7.51 (d, $J = 16.1$ Hz, 1H), 7.28 – 7.23 (m, 1H), 6.39 (d, $J = 16.1$ Hz, 1H), 1.48 (s, 9H). ^{13}C -NMR (101 MHz, CDCl_3) δ 165.61, 150.90, 149.57, 139.77, 134.20, 130.46, 123.58, 122.49, 81.00, 28.30.

(E)-3-styrylpyridine^[9a] (10ac) White solids. Yield 145 mg 80% (Catalyst **C1**), 150.4 mg 83% (Catalyst **C2**); δ (400 MHz, CDCl_3) 8.72 (s, 1H), 8.48 (d, $J = 6.3$ Hz, 1H), 7.82 (dt, $J = 7.9, 1.7$ Hz, 1H), 7.56 – 7.49 (m, 2H), 7.37 (t, $J = 7.8$ Hz, 2H), 7.32 – 7.25 (m, 2H), 7.17 – 7.01 (m, 2H). ^{13}C -NMR (126 MHz, CDCl_3) δ 139.20, 136.30, 132.24, 131.80, 129.56, 128.87, 128.54, 126.85, 126.13, 122.03, 115.00.

Gram-scale synthesis of the UV-B sunscreen agent octinoxate

In a 50 mL round-bottomed flask were placed 0.001 mol% of **C2** catalyst, 1-bromo-4-methoxybenzene (10 mmol) and 2-ethylhexyl acrylate (12 mmol), 20 mmol of Et_3N and 20 mL of NMP. The reaction flask was heated at 140 °C for 8 h in an oil bath. The reaction was monitored by TLC, the reaction mixture was cooled to ambient temperature, H_2O (5 mL) was added and the organic layer was extracted with CH_2Cl_2 (3x15 mL). The combined organic layers were dried with magnesium sulphate and concentrated. The crude product was purified by column chromatography (ethyl acetate-hexane). ^1H NMR and ^{13}C NMR data are depicted in supporting information Figures S157-158.

2-ethylhexyl(E)-3-(4-methoxyphenyl)acrylate (12)^[9a] Colorless oil. 2.11g 73% (Catalyst **C2**); ^1H NMR (400 MHz, CDCl_3) δ 7.62 (d, $J = 16.0$ Hz, 1H), 7.46 (d, $J = 8.1$ Hz, 2H), 6.88 (d, $J = 8.6$ Hz, 2H), 6.30 (d, $J = 16.0$ Hz, 1H), 4.11-4.07 (dd, $J = 5.9, 2.6$ Hz, 2H), 3.81 (s, 3H), 1.65- 1.59 (m, 6.0 Hz, 1H), 1.43-1.29 (m, 9H), 0.94 – 0.85 (m, 7H). ^{13}C NMR (101 MHz, CDCl_3) δ 167.65, 161.39, 144.24, 129.79, 127.29, 115.87, 114.32, 66.89, 55.46, 38.96, 30.56, 29.05, 23.93, 23.08, 14.20, 11.11.

XPS analysis

A sample for TEM analysis was prepared as follows After $\text{C}_{sp^2}\text{-H}$ arylation of imidazoles of (0.0005 mmol) **C2**, of 1-methyl-1H-imidazole (1.0 mmol), 4-bromo benzaldehyde (1 mmol), K_2CO_3 (2 mmol), pivalic acid (0.03 mmol) DMA (2.0 mL), 130 °C, reaction mixture was dropped onto a glass slide. Then the sample was dried under air. The resulting sample was then examined for XPS analysis.

For Mizoroki-Heck reactions, 0.001 mol% of pallacycles catalyst **C2**, 4-bromo benzaldehyde 1 mmol of, 1.2 mmol of methyl acrylate, 2 mmol of Et_3N and 2.0 mL of NMP stirred at 140 °C for 8 h in an oil bath. After completion of the reaction, the mixture was dropped onto a glass slide. Glass slide was dried under air. The resulting sample was then examined for XPS analysis.

FE-SEM and TEM analysis

A sample for TEM analysis was prepared as follows $\text{C}_{sp^2}\text{-H}$ arylation of 1-methyl-1H-imidazole in the presence of catalyst **C2**, under standard condition, the reaction mixture was diluted with DMA. Then one drop was dropped onto a copper grid and dried under air. The resulting sample was then examined for TEM analysis. A similar process was also followed for the

FULL PAPER

sample preparation of Mizoroki-Heck reaction catalyzed by **C2** for TEM analysis.

Hg poisoning test

To carry out the Hg poisoning test, catalyst **C2** (0.05 mol%) was stirred with 1 drop of Hg in an oven-dried RB. After that, 1-methyl-1H-imidazole (1.0 mmol), 4-bromobenzaldehyde (1 mmol), K₂CO₃ (2 mmol), pivalic acid (0.03 mmol) DMA (2.0 mL), 130 °C were added to the flask and reaction was carried out under optimum conditions. Reaction progress was monitored with TLC. The same procedure was followed in case of Mizoroki-Heck reactions, 1 drop of Hg in an oven-dried RB followed by 0.001 mol% of palladacycles catalyst **C2**, bromobenzene 1 mmol, 1.2 mmol of methyl acrylate, 2 mmol of Et₃N and 2.0 mL of NMP stirred at 140 °C for 8 h in an oil bath. Reaction progress was monitored with TLC.

PPh₃ poisoning test

PPh₃ (5 mol%) was taken in a reaction flask before the addition of the reactants (1-methyl-1H-imidazole, 4-bromobenzaldehyde or methyl acrylate and bromobenzene). After that, the C_{sp}²-H arylation of imidazoles reaction or Mizoroki-Heck reactions was carried out under optimum conditions. After carrying out the reaction for the optimum time, the yield of the coupled product was 31 and 41%, respectively.

Supporting information summary

Supporting information contains the experimental section, NMR, MS, UV-Visible spectral data. X-ray crystal structural data deposited in the Cambridge Crystallographic Data Centre and the deposition number for Catalyst **C1** is CCDC 1963207, **C2** is CCDC 1963208, **C3** is CCDC 1963209 and **C4** is CCDC 1963210.

Acknowledgements

KG is thankful to CSIR, New Delhi 01(2942)/18/EMR-II dated 01-05-2018) for financial assistance. AM, OS, and AM are also grateful to MHRD for fellowship. SS is thankful to DST/INSPIRE Fellowship/2017/IF170967 for financial support. We thank Prof. Marilyn Olmstead for her help in crystallographic data.

Conflict of interest

The authors declare no conflict of interest.

Keywords: Palladacycles • Direct arylation • Mizoroki-Heck • Pd(0) Nanoparticle • Octinoxate

[1] (a) E. Alacid, D. A. Alonso, L. Botella, C. Nájera, M. C. Pacheco, *Chem. Rec.* **2006**, *6*, 117–132. (b) D. Roy, Y. Uozumi, *Adv. Synth. Catal.* **2018**, *360*,

602–625 (c) M. Lamblin, L. Nassar-Hardy, J. C. Hierso, E. Fouquet, F. X. Felpin, *Adv. Synth. Catal.* **2010**, *352*, 33–79. (d) I. G. Jung, S. U. Son, K. H. Park, K. Chung, J. W. Lee, Y. K. Chung, *Organometallics* **2003**, *22*, 4715–4720.

[2] J. Magano, J. R. Dunetz, *Chem. Rev.* **2011**, *111*, 2177–2250.

[3] (a) S. O. Ojwach, A. O. Ogwenyo, M. P. Akerman, *Catal. Sci. Technol.* **2016**, *6*, 5069–5078.

(b) E. Baráth, *Catalysts* **2018**, *8*, 671–696.

[4] (a) Y. Huang, S. A. Y. Pullarkat, Li, P. H. Leung, *Chem. Commun.* **2010**, *46*, 6950–6952. (b) S. A. Pullarkat, *Synthesis* **2016**, *48*, 493–503.

[5] T. Gensch, M. N. Hopkinson, F. Glorius, J. Wencel-Delord, *Chem. Soc. Rev.* **2016**, *45*, 2900–2936.

[6] X. Marset, S. De Gea, G. J. Guillena, D. Ramón, *ACS Sustainable Chem. Eng.* **2018**, *6*, 5743–5748.

[7] (a) L. Jin, W. Wei, N. B. Sun, Hu, Z. Shen, X. Hu, *Org. Chem. Front.* **2018**, *5*, 2484–2491 (b) M. Chen, K. Wu, C. Chen, *Eur. J. Inorg. Chem.* **2012**, *2012*, 720–726. (c) P. Majumder, P. Paul, P. Sengupta, S. Bhattacharya, *J. Organomet. Chem.* **2013**, *736*, 1–8. (d) A. Maji, A. Singh, A. Mohanty, P. K. Maji, K. Ghosh, *Dalton Trans.*, **2019**, *48*, 17083–17096.

[8] J. L. Bolliger, C. M. Frech, *Adv. Synth. Catal.* **2009**, *351*, 891–902.

[9] (a) G. Hamasaka, S. Ichii, Y. Uozumi, *Adv. Synth. Catal.* **2018**, *360*, 1833–1840 (b) M. S. Yoon, D. Ryu, J. Kim, K. H. Ahn, *Organometallics* **2006**, *25*, 2409–2411 (c) Q. Luo, J. Z. Tan, Li, Y. Qin, L. Ma, D. Xiao, *Dalton Trans.* **2011**, *40*, 3601–3609 (d) Q. Mahmood, E. Yue, W. Zhang, G. A. T. Solan, Liang, W. H. Sun, *Org. Chem. Front.* **2016**, *3*, 1668–1679.

[10] (a) Q. Shen, J. F. Hartwig, *Org. Lett.* **2008**, *10*, 4109–4112 (b) B. P. Fors, S. L. Buchwald, *J. Am. Chem. Soc.* **2011**, *132*, 15914–15917.

[11] (a) B. Narasimhan, D. Sharma, P. Kumar, *Med. Chem. Res.* **2011**, *20*, 1119–1140 (b) S. Khabnadideh, Z. Rezaei, A. Khalafi-Nezhad, R. Bahrinajafi, R. Mohamadi, A. A. Farrokhriz, *Bioorganic Med. Chem. Lett.* **2003**, *13*, 2863–2865.

[12] (a) F. Shibahara, E. Yamaguchi, T. Murai, *J. Org. Chem.* **2011**, *76*, 2680–2693 (b) X. X. He, Y. Li, B. B. Ma, Z. Ke, F. S. Liu, *Organometallics* **2016**, *35*, 2655–2663 (c) H. H. Li, R. Maitra, Y. T. Kuo, J. H. Chen, C. H. Hu, H. M. Lee, *Appl. Organomet. Chem.* **2018**, *32*, 3956.

[13] (a) P. V. Kumar, W. S. Lin, J. S. Shen, D. Nandi, H. M. Lee, *Organometallics* **2011**, *30*, 5160–5169 (b) Y. Li, X. Yu, Y. Wang, H. Fu, X. Zheng, H. Chen, R. Li, *Organometallics* **2018**, *37*, 979–988.

[14] S.; Guo, H. V. Huynh, *Organometallics* **2014**, *33*, 2004–2011.

[15] (a) L. González-Sebastián and D. Morales-Morales, *J. Organomet. Chem.*, **2019**, *893*, 39–51. (b) M. Asay and D. Morales-Morales, *Dalton Trans.*, **2015**, *44*, 17432–17447. (c) H. Valdés, M. A. García-Eleno, D. Canseco-Gonzalez and D. Morales-Morales, *ChemCatChem*, **2018**, *10*, 3136–3172.

[16] A. S. Sigeev, A. S. Peregudov, A. V. Cheprakov, I. P. Beletskaya, *Adv. Synth. Catal.* **2015**, *357*, 417–429.

[17] A. E. Wang, J. H. Xie, L. X. Wang, Q. L. Zhou, *Tetrahedron* **2005**, *61*, 259–266.

[18] J.-Y. Lee, J.-S. Shen, R.-J. Tzeng, I.-C. Lu, J.-H. Lii, C.-H. Hu, H. M. Lee, *Dalton Trans.* **2016**, *45*, 10375–10388.

[19] (a) E. Peris, R. H. Crabtree, *Chem. Soc. Rev.* **2018**, *47*, 1959–1968 (b) J. L. Niu, X. Q. Hao, J. F. Gong, M. P. Song, *Dalton. Trans.* **2011**, *40*, 5135–5150.

[20] (a) A. Togni, C. Breutel, A. Schnyder, F. Spindler, H. Landert, A. Tijani,

FULL PAPER

- J. Am. Chem. Soc.* **1994**, *116*, 4062–4066 (b) H. U. Blaser, W. Brieden, B. Pugin, F. Spindler, M. Studer, A. Togni, *Top. Catal.* **2002**, *19*, 3–16.
- [21] (a) B.S. Sathe, E. Jaychandran, V. A. Jagtap, S. D. Deshmukh, *Der Pharm. Chem.*, **2011**, *3*, 305–309. (b) K. Wittine, M. Stipković Babić, D. Makuc, J. Plavec, S. Kraljević Pavelić, M. Sedić, K. Pavelić, P. Leyssen, J. Neyts, J. Balzarini and M. Mintas, *Bioorganic Med. Chem.*, **2012**, *20*, 3675–3685 (c) J. Liu, H. Lee, M. Huesca, A. Young C. Allen *Cancer Chemother. Pharmacol.* **2006**, *58*, 306. (d) D. Parthiban and R. J. Karunakaran, *Orient. J. Chem.*, **2018**, *34*, 3004–3015.
- [22] (a) J. Gising, M. T. Nilsson, L. R. Odell, S. Yahiaoui, M. Lindh, H. Iyer, A. M. Sinha, B. R. Srinivasa, M. Larhed, S. L. Mowbray and A. Karlén, *J. Med. Chem.*, **2012**, *55*, 2894–2898. (b) R. Selig, M. Goettert, V. Schattel, D. Schollmeyer, W. Albrecht and S. Laufer, *J. Med. Chem.*, **2012**, *55*, 8429–8439.
- [23] (a) J. A. Shah and B. M. Bhanage, eds. A. R. Kapdi and D. B. T. P. Maiti, *Palladacycles Catalysis and Beyond* chapter 2 Elsevier, **2019**, pp. 327–342. (b) P. Y. Choy, X. He and F. Y. Kwong, eds. A. R. Kapdi and D. B. T.-P. Maiti, *Palladacycles Catalysis and Beyond* Chapter 8 Elsevier, **2019**, pp. 21–173.
- [24] (a) K. Yu, W. Sommer, J. M. Richardson, M. Weck and C. W. Jones, *Adv. Synth. Catal.*, **2005**, *347*, 161–171. (b) M. R. Eberhard, *Org. Lett.*, **2004**, *6*, 2125–2128. (c) W. J. Sommer, K. Yu, J. S. Sears, Y. Ji, X. Zheng, R. J. Davis, C. David Sherrill, C. W. Jones and M. Weck, *Organometallics*, **2005**, *24*, 4351–4361.
- [25] (a) S. Rath, A. Maji, O. Singh, K. Ghosh, *J. Indian Chem. Soc.* **2015**, *92*, 1913–1924 (b) S. Rath, A. Maji, U. P. Singh, K. Ghosh, *Inorganica Chim. Acta* **2019**, *486*, 261–273 (c) A. Maji, O. Singh, S. Rath, U. P. Singh, K. Ghosh, *ChemistrySelect* **2019**, *4*, 7246–7259.
- [26] N. Conde, R. SanMartin, M. T. Herrero, E. Domínguez, *Adv. Synth. Catal.* **2016**, *358*, 3283–3292.
- [27] R. Simayi, E. G. Hope, K. Singh, W. B. Cross, G. A. Solan, *J. Organomet. Chem.* **2017**, *851*, 254–264.
- [28] L. Jin, W. Wei, N. Sun, B. Hu, Z. Shen, X. Hu, *Org. Chem. Front.* **2018**, *5*, 2484–2491.
- [29] (a) M. Lafrance K. Fagnou, *J. Am. Chem. Soc.* **2006**, *128*, 16496–16497; L. M. Pardo, A. M. Prendergast, M.T. Nolan, E. Ó. Muimhneacháin, G. P. McGlacken, *Eur. J. Org. Chem.* **2015**, 3540–3550
- [30] L. Q. Hu, R. L. Deng, Y. F. Li, C. J. Zeng, D. S. Shen, F. S. Liu, *Organometallics* **2018**, *37*, 214–226.
- [31] Y. Lee, H. Zseng, Z. Tsai, Y. Su, C. Hu, H. M. Lee, *Organometallics* **2019**, *38*, 805–815.
- [32] R. Bhaskar, A. K. Sharma, A. K. Singh, *Organometallics* **2018**, *37*, 2669–2681.
- [33] S. Mao, X. Shi, J.-F. Soulé, H. Doucet, *Adv. Synth. Catal.* **2018**, *360*, 3306–3317.
- [34] Y. Li, X. Yu, Y. Wang, H. Fu, X. Zheng, H. Chen, R. Li, *Organometallics* **2018**, *37*, 979–988.
- [35] A. Mollar-Cuni, D. Ventura-Espinosa, S. Martín, Á. Mayoral, P. Borja, J. A. Mata, *ACS Omega* **2018**, *3*, 15217–15228.
- [36] Y. Zhang, X. He, J. Ouyang, H. Yang, *Sci. Rep.* **2013**, *3*, 1–6.
- [37] (a) F. M. Chen, F. D. Huang, X. Y. Yao, T. Li, F. S. Liu, *Org. Chem. Front.* **2017**, *4*, 2336–2342 (b) S. I. Gorelsky, *Coord. Chem. Rev.* **2013**, *257*, 153–164.
- [38] K. Takenaka, Y. Uozumi, *Adv. Synth. Catal.* **2004**, *346*, 1693–1696.
- [39] (a) M. P. Singh, F. Saleem, G. K. Rao, S. Kumar, H. Joshi and A. K. Singh, *Dalton Trans.*, **2016**, *45*, 6718–6725. (b) N. Selander and K. J. Szabó, *Chem. Rev.*, **2011**, *111*, 2048–2076.
- [40] (a) J. Dupont, M. Pfeffer, *Palladacycles* Eds.; Wiley-VCH: Weinheim, Germany, **2008** (b) I. P. Beletskaya, A. V. Cheprakov, *J. Organomet. Chem.* **2004**, *689*, 4055. (c) F. Saleem, G. K. Rao, A. Kumar, S. Kumar, M. P. Singh and A. K. Singh, *RSC Adv.*, **2014**, *4*, 56102–56111.
- [41] (a) Á. Molnár, *Chem. Rev.* **2011**, *111*, 2251–2320 (b) C. M. Crudden, M. Sateesh, R. Lewis, *J. Am. Chem. Soc.* **2005**, *127*, 10045–10050.
- [42] M. R. Eberhard, *Org. Lett.* **2004**, *6*, 2125–2128 (b) N. T. S. Phan, M. V. D. Sluys, C. W. Jones, *Adv. Synth. Catal.* **2006**, *348*, 609 – 679.
- [43] G. M. Sheldrick, *Acta Cryst. A* **1990**, *46*, 467–473.
- [44] G. M. Sheldrick, *SHELXTL NT 2000 Version 6.12, Reference Manual*, University of Göttingen, Pergamon, New York, 1980.
- [45] O.V. Dolomanov, L. J. Bourhis, R. J. Gildea, J. A. K. Howard, H. Puschmann, *J. Appl. Cryst.* **2009**, *42*, 339–341.
- [46] B. Klaus, *Diamond, Version 1.2 c*, University of Bonn, Germany, 1999.
- [47] F. Panahi, N. Zarnaghash, A. Khalafi-Nezhad, *New J. Chem.* **2016**, *40*, 1250–1255.

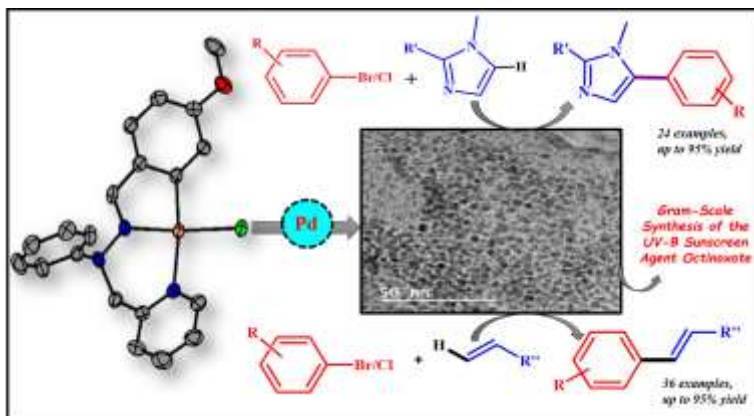
FULL PAPER

FULL PAPER

Author(s), Corresponding Author(s)*

Page No. – Page No.

Title



Palladium Catalysts **C1**–**C4** derived from unsymmetrical pincer-type ligands were design and synthesized and were characterized by different spectroscopic methods. Crystal structures of **C1**–**C4** were established. These Catalysts (**C1**–**C4**) were employed for C_{sp}²-H arylation of imidazoles derivatives and Mizoroki-Heck reactions. Grams scale synthesis of UV-B sunscreen agent octinoxate.